Heliyon 10 (2024) e34832

Contents lists available at ScienceDirect

Heliyon

journal homepage: www.cell.com/heliyon

Research article

# Estimation of return dates and return levels of extreme rainfall in the city of Douala, Cameroon

Calvin Padji [a,*], Cyrille Meukaleuni [b], Cyrille Mezoue Adiang [a,c], Daniel Bongue [d], David Monkam [a]

[a] Department of Physics, Faculty of Science, University of Douala, P.O. Box:24157, Douala, Cameroon
[b] University Institute of the Coast, P.O. Box:3001, Douala, Cameroon
[c] Laboratory of Energy, Materials, Modelling and Method, National Higher Polytechnic School of Douala, University of Douala, P.O. Box:2701, Douala, Cameroon
[d] CEPAMOQ, Faculty of Science, University of Douala, 8580, Douala, Cameroon

ARTICLE INFO

*Keywords:*
Extreme precipitation
Floods
Return period
Return dates
Return level
Confidence interval

ABSTRACT

The problem of extreme phenomena with a more precise estimation of their return periods for early warnings, notably to preserve the safety of populations and properties, arises all over the world. This work develops another aspect in the estimation of Return Levels (RLs) and Return Periods (RPs) of extreme precipitation in particular and natural risk in general. In particular, it gives the Return Dates (RDs) with their Confidence Intervals (CIs). The RPs, the RLs and their CIs for extreme rainfall were also investigated. These estimates were made by approaching the peak over a threshold chosen by the Generalized Pareto Distribution (GPD). The CIs of RPs and RLs were determined by the Delta method. The daily rainfall data used were obtained from the data of the synoptic report for the period 2011 to 2021 for the Douala weather station (more details can be found on http://www.ogimet.com/guia.phtml.en). To validate the methods used, real cases of floods occurred in Douala city were considered: for example, a local press compiled flood dates and mentioned that a flood occurred on the April 16, 2013 in this city. Following the data of synoptic report, the corresponding amount of rainfall was around 150 mm. The results obtained have shown a RD on the August 12, 2014. The confidence intervals of return levels and return dates determined by the Delta method were [131.66, 168.456] and [June 23, 2014, January 02, 2015], respectively. These results are in agreement with the data of synoptic report since the rainfall amounts was 132.2 mm (belonging to the confidence interval of return levels), on the August 11, 2014 (belonging to the confidence interval of return dates). These predictions of RDs and RLs with their CIs, at reasonable time scales, can help for efficient management of floods and thus, improve early warnings for safety of populations and goods.

## 1. Introduction

Floods are the natural or artificial and temporary submersion of a territorial space. They are the leading cause of disasters worldwide [1–4]. Indeed, these disasters are the most recurrent and have a devastating effect on human lives [5]. Historical analysis of this natural phenomenon shows that it develops over time in the world. For example, 3713 geographic flood centers were registered

* Corresponding author.
*E-mail address:* padjicalvin@gmail.com (C. Padji).

https://doi.org/10.1016/j.heliyon.2024.e34832
Received 12 February 2024; Received in revised form 16 July 2024; Accepted 17 July 2024
Available online 18 July 2024

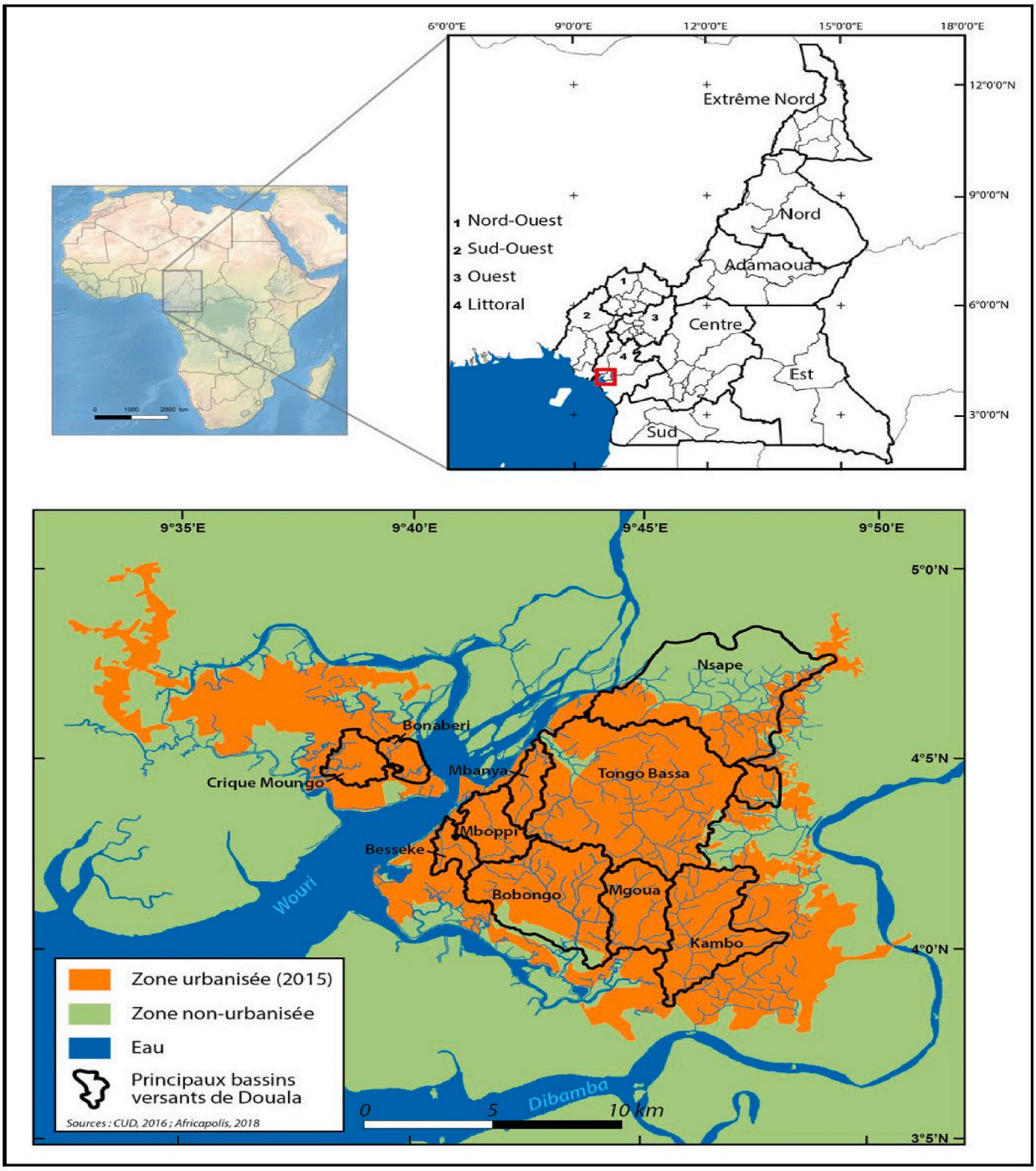


**Fig. 1.** Geographical location of the city of Douala, the Urban Zone and the main watersheds in the map of Africa and Cameroon (source: https://journals.openedition.org/physio-geo/docannexe/image/8038/img-1.jpg).

from 1985 to 2010, while 4536 were registered worldwide in 2017 (see http://floodobservatory.colorado.edu). This reflects an increase of 823 geographic flood centers after 7 years. The Center for Research on the Epidemiology of Disasters (CRED) estimates that an average of 37 catastrophic floods per year have been recorded worldwide, in the space of 113 years, 1900–2013 [6]. These estimated values concern different continents and are therefore distributed in almost all countries of the world. It is the case of the European continent whose NatCatService database reveals that 1500 floods and wet mass movements have occurred in the countries of the European Economic Area during the period of 1980–2013 (https://natcatservice.munichre.com/). The European Environment Agency

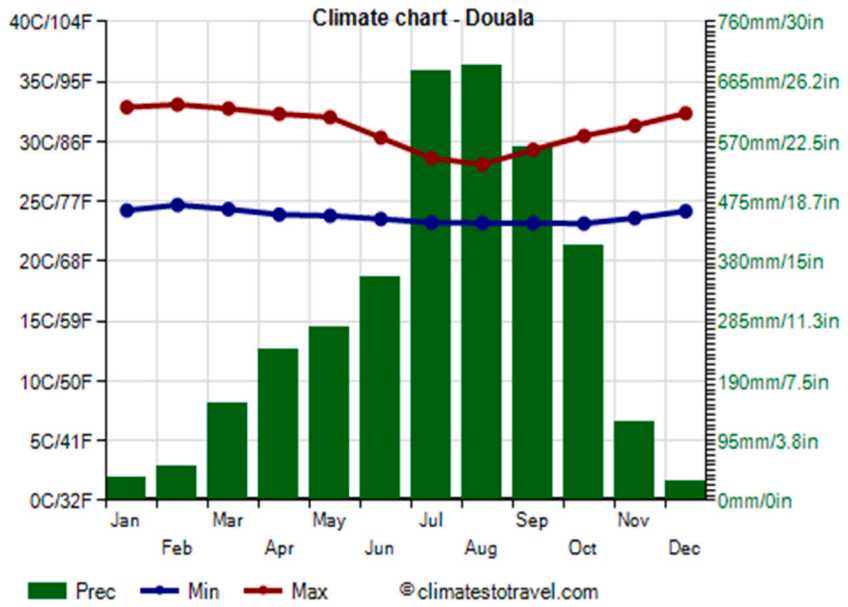


**Fig. 2.** Graph of the climate of the city of Douala (precipitation (mm) on the right and temperature ($^{o}$C) on the left) for each month from 1991 to 2020. (Source: https://www.climatestotravel.com/climate/cameroon/douala).

also estimates that more than 4700 deaths and direct economic losses worth more than 150 billion Euros are caused by floods [7]. This is a global problem and the African continent is also concerned.

The African continent is the most vulnerable region to hydro-climatic risks in the world [8,9]. This vulnerability is increased by the combination of several factors such as endemic poverty, poor governance, access to capital, inadequate infrastructure and technology, ecosystem degradation, disasters and complex conflicts [10]. In addition, inefficient solid waste collection systems, the extension of buildings in flood-prone areas and modest sewage networks, are also factors that exacerbate the danger. This leads to reinforce the predictable effect of flood risks on the issues (highly impoverished urban populations) [11]. Between June and September 2009, West Africa had more than 600 thousand people affected by the floods; they then caused human losses and material damage estimated at 2.442 million CFA francs [12]. These phenomena being very present in Africa, constitute a real problem for the people of Cameroon in general and its economic capital, Douala, in particular. Several experts considered floods as the most frequent natural disaster in Cameroon.

Indeed, according to studies published in 2016 by CRED, 367,276 people were victims of floods in Cameroon between 2007 and 2015 [13]. Due to its geographical location, the city of Douala (coastal city built on the estuary of the Wouri River) is an excellent customer of flood phenomena. For example, 34 cases of flooding were recorded in this city between 1980 and 2018 [7]. Its flat terrain, under flushed water table, density of its hydrographic network and abundant rainfall (about 4000 mm per year), are the factors that predispose Douala city to the risk of flooding. Similarly, almost continuous rainfall throughout the year increases the probability of flood risk to 80 % during the high rainy season from June to September. Even the driest months (November, December and January) have rainfall of nearly 50 mm [14,15]. The period 2000–2010 report 100 deaths and significant damage (material, human etc.) caused by flooding [6].

The challenge today is to find methods that contribute to reduce the vulnerability of the populations to these disasters.

Therefore, several initiatives are taken. Policymakers have begun building drains. Also, scientific documents have been produced in order to explain on the one hand and to predict on the other hand, the risk of flooding in this city. This is the case of the work of [7], making a temporal analysis of the representation of flood risk in Douala over the period from 1980 to 2018, and those of [16], calculating the return times (RTs) of extreme precipitation on a monthly accumulation of precipitation. Although these different works are very interesting, flooding problems remain topical and difficult to manage in the city of Douala. Indeed, the work of [16], which determined the RTs of extreme precipitation to above 80th year, does not constitute a real warning system for people affected by the flood in Douala. Several others works also gave RTs of for multiple decennials, more than 50 years [17–22]. For examples, 40th year, 50th year and 60th year are time limit and cannot be easily verified at human time scale. Furthermore, these works did not give neither the dates, nor the time intervals of the return of the extreme phenomena.

Given also that natural hazards in general and flooding in particular are global phenomena that affect everyone, several works have been carried out to try to alert populations to the most violent events to enable them to be managed. In most cases, these studies estimate the return periods for the extreme values of the parameters causing the risks (temperatures, rainfall, violent winds, etc). Among others, we have the work of [23], who conducted a study in the Pra River Catchment in Ghana, West Africa, estimating the maximum duration and return periods of rainfall and flooding using the Gumbe theory of extremes. The main results reveal that an increase in the magnitude of the consecutive wet day observed in the Centre of the Catchment had a maximum of around 30 days for

**Table 1**
Average monthly rainfall in the city of Douala from 1991 to 2020. (Source: www.climatsetvoyage.com).

| Month | Quantity (mm) | Days |
|---|---|---|
| **January** | **35** | **5** |
| **February** | **55** | **9** |
| **March** | **155** | **15** |
| **April** | **240** | **18** |
| **May** | **275** | **21** |
| **June** | **355** | **23** |
| **July** | **680** | **27** |
| **August** | **690** | **30** |
| **September** | **560** | **26** |
| **October** | **405** | **24** |
| **November** | **125** | **12** |
| **December** | **30** | **5** |
| **Year** | **3605** | **215** |

the 100-year return period, while lower flood volumes had between 50 % and 100 % higher recurrence for a 1 to 2-year return period; [24], which evaluated the performance of 4 regional climate models (REgional MOdel (REMO2009), High-Resolution Hamburg Climate Model 5 (HIRAM5), Climate Limited-Area Modelling Community (CCLM4-8) and Rossby Center Regional Atmospheric Model (RCA4)) in simulating precipitation and air temperature in south-west Ethiopia. They found that the Regeniax climate models did not simulate temperature and rainfall maxima. They are biased towards a warm climate zone in the simulation of maximum air temperature compared with the simulation of minimum air temperature. However, they indicate that REMO2009 performance well in simulating maximum and minimum temperatures. HIRAM5 overestimates the return period of extreme rainfall events; [25], characterized in the city of Niamey, Niger extreme rainfall in the face of climate change and rapid population growth using stationary and non-stationary POT. They found that rainfall of 20 mm over 3 h could be considered extreme rainfall by 2040; [26], who carry out frequency and trend analyses of annual peak flows in the lower Mekong basin. They use Log-Pearson Type-III and Gumbel Extreme Value Type-I methods to estimate the return periods of mean annual flows ($Q_m$), major floods ($Q_{lf}$) and maximum annual peak flow ($Q_{max}$). Goodness-of-fit tests showed that Log-Pearson Type-III (LP-III) is the better distribution for the Mekong maximum annual series than Gumbel Extreme Value Type-I (GEVI) and therefore LP-III gives confidence in the estimation of return periods and recurrence intervals of mean annual discharge, large floods ($Q_{lf}$) and maximum annual peak discharge ($Q_{max}$); [27], which assess the performance of the CMIP6 model in predicting extreme rainfall in the Awash basin in Ethiopia. They show that the models as a whole overestimate the return periods of extreme rainfall and that the Generalized Extreme Value Distribution is suitable for estimating extreme values accurately. They also found that the GFDL-ESM4 and BCC-CSM2-MR models were the most accurate at simulating extreme rainfall; [28], who estimate regional quantiles using the flood index procedure on an extreme wind site. They attempted to find the regional distribution of maximum wind frequencies and to predict the return of extreme wind elements in the future; [29], who have carried out a detailed study on the quantification and modelling of drought characteristics using different families of copulas. Through their work, they predict a severe drought in the region, with longer return periods over a specific period of time; [30], has been working on the prediction of extreme rainfall in the Bangkok metropolitan region. He finds that periods of heavy/very heavy rainfall in October will increase in the years 2070–2098 compared to the years 1980–2009 in the region; [31], studied the temporal variability of droughts on a national scale in the Kingdom of Eswatini; The main results obtained were that moderate droughts reoccur every 4–5 years and extreme droughts every 13–21 years. These results were obtained using of the standardised rainfall index calculation method [32];, which project extreme temperatures by assessing the history of changes in the Baluchistan region of Pakistan using extreme value theory. They evaluate the behaviour of minimum and maximum temperatures over a return period of 100 years in the near (2041–2070) and distant (2071–2100) future. The assessment of historical temperature trends suggests that maximum temperatures generally increase on an annual scale and give mixed signals on a seasonal scale, while minimum temperatures have given mixed signals on an annual and seasonal scale.

Analysing the works presented above concerning the prediction of extreme values, we ~~note~~ that they lack validation of the results by real climatic phenomena observed (for example, floods caused by extreme precipitations in a given region). In addition, SOTA methods (models that predict future values on the basis of past data) like REMO2009, HIRAM5, CCLM4-8, RCA4 [24], CMIP6, GFDL-ESM4, BCC-CSM2-MR [27], overestimate the return periods of extreme precipitation events and do not provide return dates or confidence intervals for predicted extremes. These works also present models that are effective in predicting future data in one region and seem less effective in the other. Indeed, when one predicts an extreme value in the future with a return period during which the value can be recorded, one may find a different value at that period. So, when forecasting extreme climatic parameters, it is important to give the confidence interval at a given probability of its return level. It is also preferable to add an estimate of the return date and a confidence interval of the return date at a given probability of the predicted extreme, to allow verification with real events. So, several passed works including [33–41] investigated on return periods and return values of extreme events using different methods. But none of these works has estimated the return dates of extreme values and their confidence intervals. It is therefore necessary to find a method to determine (i) the return periods and their confidence intervals, (ii) the return dates and their confidence intervals, (iii) the return levels and their confidence intervals, to contribute to a good warning system of natural and extreme risks.

Therefore, in this work we propose to determine the Return Periods (RPs), the Return Dates (RDs) and the Return Levels (RLs) with

their Confidence Intervals (CIs) for extreme precipitations in Douala city. The results will be validated through past extreme rainfalls (floods) identified in Douala. Their validation will provide insight for future risk prediction and hopefully, will serve as an early warning tool against danger and for climatic change adaptation. Although the method used is applied using daily rainfall for the Douala city, it can also be applied to other regions of the world and other climatic parameters.

The next section describes data and methods. Section 3 presents results and discussions. A conclusion is provided in section 4.

## 2. Data and methods

### 2.1. Study domain

Douala, the economic hub of Cameroon, is located southwest of Cameroon on the coast of the Gulf of Guinea near the sea, and at the foot of the mountain range of that country. It is on longitude 9.7° E and latitude 4.0° N (Fig. 1). This figure locates not only the city of Douala, but also the urban area and its main watersheds (http://journals.openedition.org/physio-geo/docannexe/image/8038/img-1.jpg). Also, the climate in this city is tropical warm with intermittent rains [42–44]. This city has a dry season from December to February and a long rainy season from March to November, with very abundant rains from June to October (see Fig. 2), as it is directly influenced by the African monsoon. Given the abundance and frequency of rainfall, the sunshine is not very good. In this city the average temperature of the coldest month (August) is 25.6 °C, that of the hottest month (February) is 28.9 °C. Rainfall is very abundant in this part of Cameroon. They are estimated at 30 mm in the least rainy month (December) and 690 mm in the rainiest month (August), with an annual mean of about 3605 mm (Table 1). It is acceptable that extreme precipitation, encouraged by the population boom, will cause significant flooding in this locality.

### 2.2. Data

We used daily precipitations (2011–2021) acquired by synoptic reports data for Douala meteorological station (World Meteorological Organization-WMO-index of 64,910). The Ogimet weather information service stores database for all meteorological services around the whole world. It is based on WMO and the international aviation organization (ICAO) station indices. It is the case of Douala meteorological station. The daily means are based directly on climate reports (FM 71-XI), usually available during the first 10 days of the next month (see http://www.ogimet.com/guia.phtml.en for some details). These precipitations data have already been successfully used by Refs. [45,46], to estimate monthly precipitations and recently by Ref. [47], for the analysis of the diurnal to seasonal variability of solar radiation connection with rainfall in Douala, Cameroon. The authors confirm that these reports can be used with a good accuracy. Furthermore, these synoptic reports also provide data on other climatic parameters (temperature, humidity, solar radiation, wind speed and global luminance) which have also been used in several studies: [48–50], to characterize climatic variability; [42], to analyze the weather conditions and [51], to estimate global solar radiation in some regions of Cameroon. These various data are measured with frequencies of 10–15 min and in height from the ground between 3 and 10 m.

### 2.3. Methods

#### 2.3.1. Return level ( $x_m$) and return periods (m) through peak-over-threshold method

Two mathematical approaches, one based on crossing frequency [52], and the other based on extreme value theory (EVT) [53], are generally used for the study of extreme phenomena. Due to its evolution, EVT is proving to be a very important statistical discipline in the analysis of extreme values. It also intervenes as well in fields such as engineering, economics, reliability modeling and finally the environment which is the focus of our interesting [54].

In this work, we used extreme value theory (EVT). This approach refers as a whole to two fundamental statistical models for modelling and estimating extreme values. These are the Block Maxima (BM) and the Peak-Over-Threshold (POT) approaches. The POT approach is identified as the best alternative for the analysis of extreme values compared to BM [54,55]. Therefore, we used POT in this study.

Based on the theory of extreme values, peak-over-threshold (POT) consists of defining a Generalized Pareto Distribution (GPD) function. GPD contains parameters whose estimates are made by the maximum likelihood method (MLE) [1,33,35,36]. Extreme values are estimated by a probability of threshold exceedances [56–60]. This probability depends on a "u" value (to be chosen) called the threshold of exceedance, obtained using techniques such as: (i) the Mean Residual Life (MRL) which consists in representing the average of extreme values that exceed a given threshold on a graph; (ii) the graphs of scale and shape parameters according to the different thresholds that plot the modified scale and shape parameters of the GPD model, and (iii) the automatic threshold selection algorithm that provides a code for automatically choosing the threshold [61]. The POT model also makes it possible to estimate return periods RPs and return levels RLs made on the basis of the tail of the GPD, adjusted to the distributions for values exceeding the chosen threshold [62]. Moreover, these (RPs) and (RLs) are estimated from the 95 % confidence level obtained by the delta method, which is the technique for calculating confidence intervals (CIs).

The POT approach models distributions tails based on Balkema & De Haan's. [63], theorem that determines a generalized Pareto distribution function Davison, Pickands III, Smith [37,39,41,64]. by equation (1):

$$G(x)=\left\{1-\left[1+\xi\left(\frac{x-u}{\sigma}\right)\right]^{-\frac{1}{\xi}}\right\} \tag{1}$$

where u is the chosen threshold, $x$ a generic variable conditional on u ($x > u$), $\xi$ the shape parameter ($\xi \neq 0$) and σ the scale parameter ($\sigma > 0$).

If $\xi < 0$, the tail of the theoretical GPD has a large limit (beta distribution), while if $\xi > 0$, the tail of the theoretical GPD has no upper limit (Pareto distribution) and if $\xi = 0$, the GPD converges to an exponential distribution.

These parameters were estimated using the maximum likelihood method [65]. Following [54] the probabilities associated with the function G(x) are expressed by equation (2):

$$Pr\,(X > x) = Pr\,(X > u).\,(1 - G\,(x)) \tag{2}$$

where $Pr\,(X > u)$ is the probability of exceeding the estimated threshold through the number of daily precipitations exceeding threshold u divided by the total number of precipitations measured [54,66].

By the substitution of G(x) from equation (1), in equation (2), we obtain equation (3).

$$\Pr\{X > x\} = \zeta_u\left[1+\xi\left(\frac{x-u}{\sigma}\right)\right]^{-\frac{1}{\xi}} \tag{3}$$

with $\zeta_u = \Pr\{X > u\}$. Therefore, the value of RL ($x_m$) which is exceeded on average once every value of RP (m) observation is the solution of equation (4):

$$\zeta_u\left[1+\xi\left(\frac{x_m-u}{\sigma}\right)\right]^{-\frac{1}{\xi}} = \frac{1}{m} \tag{4}$$

equation (5) below is the solution of the resolution of equation (4) to obtain $x_m$ :

$$x_m = u + \frac{\sigma}{\xi}\left[(m\zeta_u)^{\xi} - 1\right] \tag{5}$$

The equation found in (4) gives the value of m by the relation (6):

$$m = \frac{\left[1+\xi\left(\frac{x_m-u}{\sigma}\right)\right]^{\frac{1}{\xi}}}{\zeta_u} \tag{6}$$

Estimation of return levels and return period requires the substitution of parameter values $(\zeta_u, \xi, \sigma)$ of relations (5) and (6) by their estimate's values $(\widehat{\zeta}_u, \widehat{\xi}, \widehat{\sigma})$. $\widehat{\xi}$ and $\widehat{\sigma}$ corresponds to maximum likelihood estimates. $\widehat{\zeta}_u = \frac{k}{n}$ is sample proportion of points exceeding u and also the maximum likelihood estimate. k represented the number of extremes above u and n sample size of distribution.

### 2.3.2. Confidence interval of RPs (m) and RLs ($x_m$) by delta method

Using formula (6) given the function m and [67] which presents the method to calculate the variance of a function, therefore the variance of m is obtained by equation (7).

$$\mathrm{var}(m) = \left(\frac{\partial m}{\partial \zeta_u}\right)^2 \mathrm{var}(\widehat{\zeta}_u) + \left(\frac{\partial m}{\partial \xi}\right)^2 \mathrm{var}(\widehat{\xi}) + \left(\frac{\partial m}{\partial \sigma}\right)^2 \mathrm{var}(\widehat{\sigma}) + 2\frac{\partial m}{\partial \xi}\frac{\partial m}{\partial \sigma}\mathrm{cov}(\widehat{\xi}, \widehat{\sigma}) \tag{7}$$

According to the standard properties of the binomial distribution [54], $Var(\widehat{\zeta}_u) \approx \widehat{\zeta}_u(1-\widehat{\zeta}_u)/n$ According to Ref. [60], for $\xi > -0.5$, Maximum likelihood estimators were asymptotically normal and the variance covariance matrix M of $(\widehat{\xi}, \widehat{\sigma})$ is given by equation (8).

$$M = \begin{pmatrix} (1+\widehat{\xi})^2 & -\widehat{\sigma}(1+\widehat{\xi}) \\ -\widehat{\sigma}(1+\widehat{\xi}) & 2\widehat{\sigma}^2(1+\widehat{\xi}) \end{pmatrix} \tag{8}$$

From M and by identically: $\mathrm{var}(\widehat{\xi}) = (1+\widehat{\xi})^2$, $\mathrm{var}(\widehat{\sigma}) = 2\widehat{\sigma}^2(1+\widehat{\xi})$ and $\mathrm{cov}(\widehat{\xi}, \widehat{\sigma}) = -\widehat{\sigma}(1+\widehat{\xi})$.

We recall that the function m is given by equation (6). equations (9)–(11) below, correspond to the partial derivatives of m by $\zeta_u, \xi$ and $\sigma$, respectively.

$$\frac{\partial m}{\partial \zeta_u} = -\frac{1}{\zeta_u^2}\left[1+\xi\left(\frac{x_m-u}{\sigma}\right)\right]^{\frac{1}{\xi}} \tag{9}$$

$$\frac{\partial m}{\partial \xi} = \frac{1}{\zeta_u}\left[1+\xi\left(\frac{x_m-u}{\sigma}\right)\right]^{\frac{1}{\xi}}\left\{-\frac{1}{\xi^2}Log\left[1+\xi\frac{x_m-u}{\sigma}\right] + \frac{1}{\xi\sigma}\left[\frac{x_m-u}{1+\xi\left(\frac{x_m-u}{\sigma}\right)}\right]\right\} \tag{10}$$

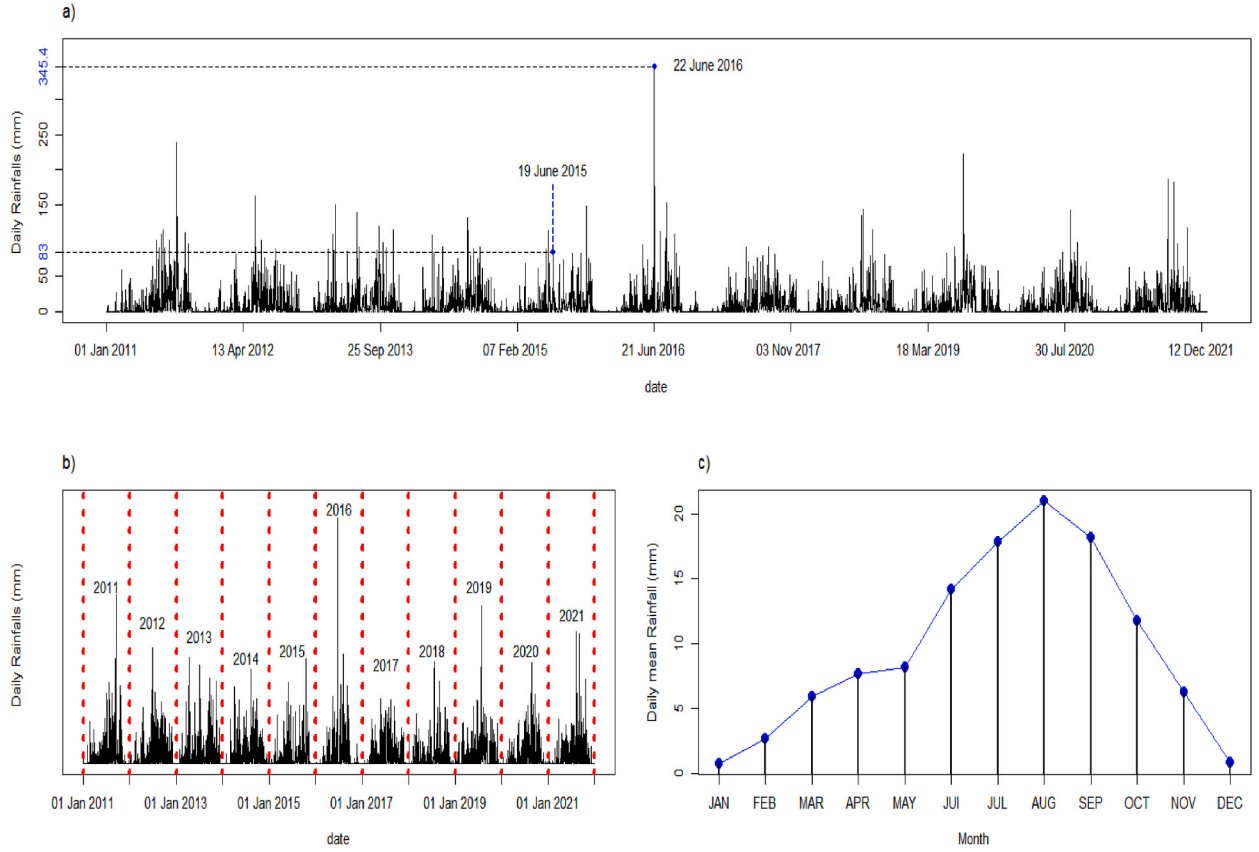


**Fig. 3.** Daily precipitation distribution (in mm) (a), a year-by-year separation of this distribution by red lines (b) and daily mean rainfall amount in each month (c) of Douala city for the period 2011 to 2021. (For interpretation of the references to colour in this figure legend, the reader is referred to the Web version of this article.)

$$\frac{\partial m}{\partial \sigma} = -\frac{x_m - u}{\sigma^2 \zeta_u}\left[1 + \xi\left(\frac{x_m - u}{\sigma}\right)\right]^{\frac{1}{\xi}} - 1 \tag{11}$$

Using formula (7) and applying the delta method to the function m, we can calculate the confidence interval (CI) of the return periods (m). The CIs are then calculated by the expression

$$\left[m - \frac{\sqrt{\mathrm{var}(m)}}{\sqrt{n}} z_{\frac{1+\alpha}{2}}, m + \frac{\sqrt{\mathrm{var}(m)}}{\sqrt{n}} z_{\frac{1+\alpha}{2}}\right] \tag{12}$$

with $\alpha$ the confidence level which takes the value of 95 % and $z_{\frac{1+\alpha}{2}}$ the quantile of order $\frac{1+\alpha}{2}$ of a reduced centered normal distribution. The calculations are identical for RL CIs. RDs CIs are calculated from RPs CIs and recorded dates for extreme precipitation.

The methods presented above were applied to daily precipitation distributions over an 11-years period (2011–2021) to determine RPs and return dates of certain extreme precipitation. On the other hand, on a breakdown by year to find the dates of return of rainfall at the origin of floods, the values of RLs and RPs are determined using relations (5) and (6).

### 2.3.3. *Return dates and confidence intervals*

*2.3.3.1. Return dates.* The return dates are determined using the following steps.

(i) We must find the number of return days of the extreme values from the return periods obtained from equation (6). There are two alternatives.
   (1) If the first digit of the decimal part of return periods is in the integer range [0, 4], then the numbers of return days are rounded down to the integer equal or less than the return periods; i.e., for return periods of 57 and 90.46, the numbers of return days are 57 days and 90 days.

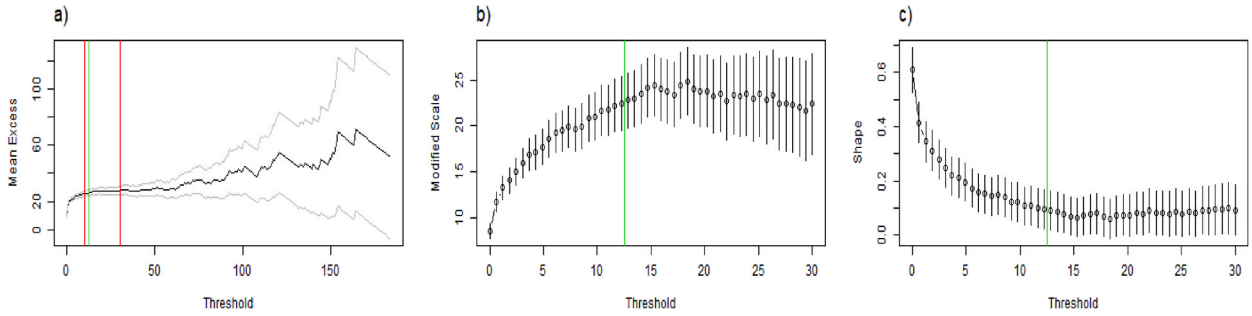


**Fig. 4.** The Mean Residual Life (MRL) plot (fig a) and the Model-Based Check (MBC) plots (fig b–c) for Douala city rainfall data from the period 2011–2021. The MBC plots show the estimates of the modified GPD model scale parameters relative to the threshold (fig b) and the estimates of the shape relative to the threshold (fig c). The dotted lines in the MRL plots and the vertical black lines in the MBC plots indicate the 95 % confidence intervals (CI).

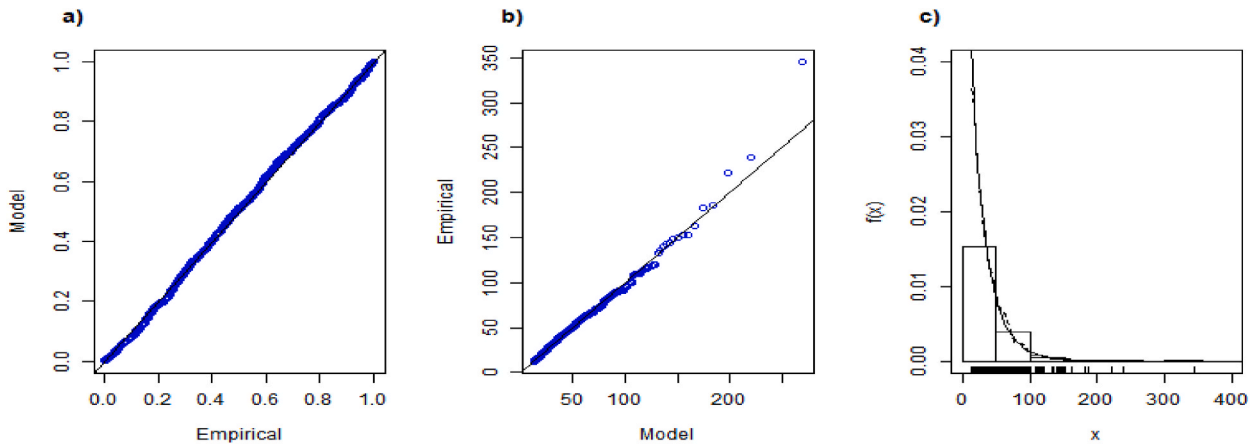


**Fig. 5.** Diagnostic plots for the generalized Pareto distribution (GPD) fitted to the 2011-21 rainfall data: this plot presents probability plots (Fig. a); quantile-quantile plots (Fig. b) and histograms of fitted data and density functions (Fig. c).

**Table 2**
GPD parameters estimated from the adjustment to a *GPD* law of the daily cumulations of precipitations in Douala city from 2011-21.

| GPD model parameters | 95 % lower CI | Estimate | 95 % upper CI | Standard Error Estimates |
|---|---|---|---|---|
| Scale | 22.781 | 23.703 | 28.225 | 1.168 |
| Shape | 0.005 | 0.095 | 0.153 | 0.036 |

(2) If this digit is in the integer range [5, 9], then the numbers of return days are rounded up to the next integer of return periods; i.e., for return periods of 57.5 and 100.742, the numbers of return days are 58 days and 101 days.

(ii) We establish the list of dates for the extreme values already obtained from POT method; i.e., on April 16, 2013, 150 mm of rainfall was recorded using POT. The date April 16, 2013 is therefore selected as a date of extreme rainfall in our list.

(iii) We then add to this date the number of return days obtained in (i) to find the return date, taking into account leap years (where February has 29 days) i.e., rainfall recorded on February 16, 2013 with a number of return days of 38 days would have a return date the March 26, 2013. But if the recording date of this precipitation is February 16, 2016, the return date will be March 25, 2016, because 2016 is a leap year.

*2.3.3.2. Confidence intervals.* The confidence intervals of dates are determined using the following steps.

(i) We must find the confidence intervals of the number of return days from confidence intervals of return periods obtained from expression (12) as follows:

(1) If the first digit of the decimal part of the lower limit of return periods confidence interval is in the integer interval [0, 9], then the lower limit of the number of return days corresponds to the round down of the integer equal or less than the lower limit of the return period confidence interval.

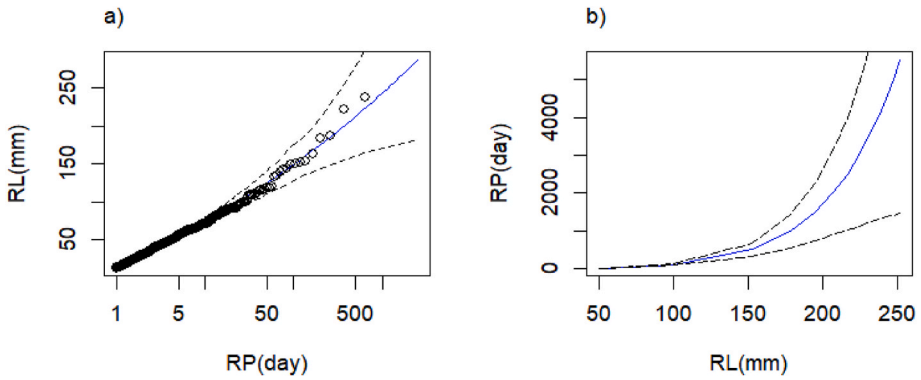


**Fig. 6.** Graph of return levels (Fig. a) and return periods (Fig. b) of extreme precipitation, cumulated daily in Douala, calculated from 2011-21 from the distribution of the GPD (black line curves of Figs. a and b) surrounded by 95 % confidence intervals (dotted curves of Figs. a and b) which are calculated by the Delta method.

**Table 3**
Estimated return levels (mm) and 95 % confidence intervals calculated by the Delta method for different return periods (days) from the adjustment of daily rainfall accumulations in Douala by the GPD model.

| RPs (day) | RLs (mm) | 95 % CIs for RLs (mm) | 95 % CIs for RPs (day) |
|---|---|---|---|
| 5 | 14.53 | [13.11, 15.94] | [5,5] |
| 7 | 22.70 | [20.99, 24.40 | [7,7] |
| 10 | 31.64 | [29.48,33.81] | [10,10] |
| 14 | 40.38 | [37.74, 42.10] | [13,13] |
| 21 | 51.26 | [48.01, 54.51] | [20,22] |
| 28 | 59.24 | [55.49, 62.10] | [26, 30] |
| 30 | 61.19 | [57.29, 65.08] | [28, 32] |
| 365 | 141.03 | [124.68, 157.38] | [255,476] |
| 730.5 | 166.77 | [143.41, 190.13] | [440,1023] |
| 1095 | 182.62 | [154.29, 210.96] | [594,1602] |
| 1421 | 193.09 | [161.22, 224.98] | [712,1423] |
| 1825 | 203.43 | [167.86, 239.00] | [841,2817] |

**Table 4**
Number of return days estimated for different maximum precipitation (mm) over each year, as well as estimated return dates of maximum rainfall and 95 % CIs using the adjustment of daily rainfall totals from 2011-21 in Douala by the *GPD model.*

| Dates of extreme rainfall in each year. | Maximum rainfall (mm) | Estimated number of return days | 95 % CIs of number of return days | 95 % CIs of RLs (mm) | Estimated dates of return of the next maximum rainfall. | 95 % CIs for RD. |
|---|---|---|---|---|---|---|
| September 13, 2011 | 238.6 | 4657 | [1313, 6910] | [188.84, 288.37] | June 15, 2023 | [April 19, 2015, August 15, 2030] |
| 27/06/2012 | 163.3 | 697 | [411, 925] | [141.11, 185.40] | June 25, 2014 | [August 13, 2013, January 09, 2015] |
| April 16, 2013 | 150 | 483 | [311, 625] | [131.66, 168.46] | August 12, 2014 | [June 23, 2014, January 02, 2015] |
| August 11, 2014 | 132.2 | 290 | [208, 362] | [118.24, 146.30] | May 28, 2015 | [March 08, 2015, August 06, 2015] |
| October 19, 2015 | 148.6 | 464 | [302, 599] | [130.61, 166.66] | January 25, 2017 | [August 17, 2016, June 17, 2017] |
| June 22, 2016 | 345.4 | 45187 | [3752,73403] | [239.69, 451.11] | March 10, 2141 | [September 01, 2025, June 10, 2217] |
| May 24, 2017 | 91.4 | 83 | [71, 94] | [84.85, 98.49] | August 15, 2017 | [August 04, 2017, August 26, 2017] |
| July 25, 2018 | 144.2 | 387 | [274, 524] | [125.85, 158.63] | August 16, 2019 | [April 26, 2019, January 01, 2020] |
| July 25, 2019 | 222.2 | 3155 | [1094, 4586] | [179.37, 265.04] | March 15, 2028 | [July 24, 2022, February 13, 2032] |
| August 21, 2020 | 142.7 | 393 | [265, 501] | [126.25, 159.31] | September 19, 2021 | [May 13, 2021, January 04, 2022] |
| August 11, 2021 | 182.2 | 1155 | [590, 1583] | [154.19, 210.22] | October 09, 2024 | [March 24, 2023, December 11, 2025] |

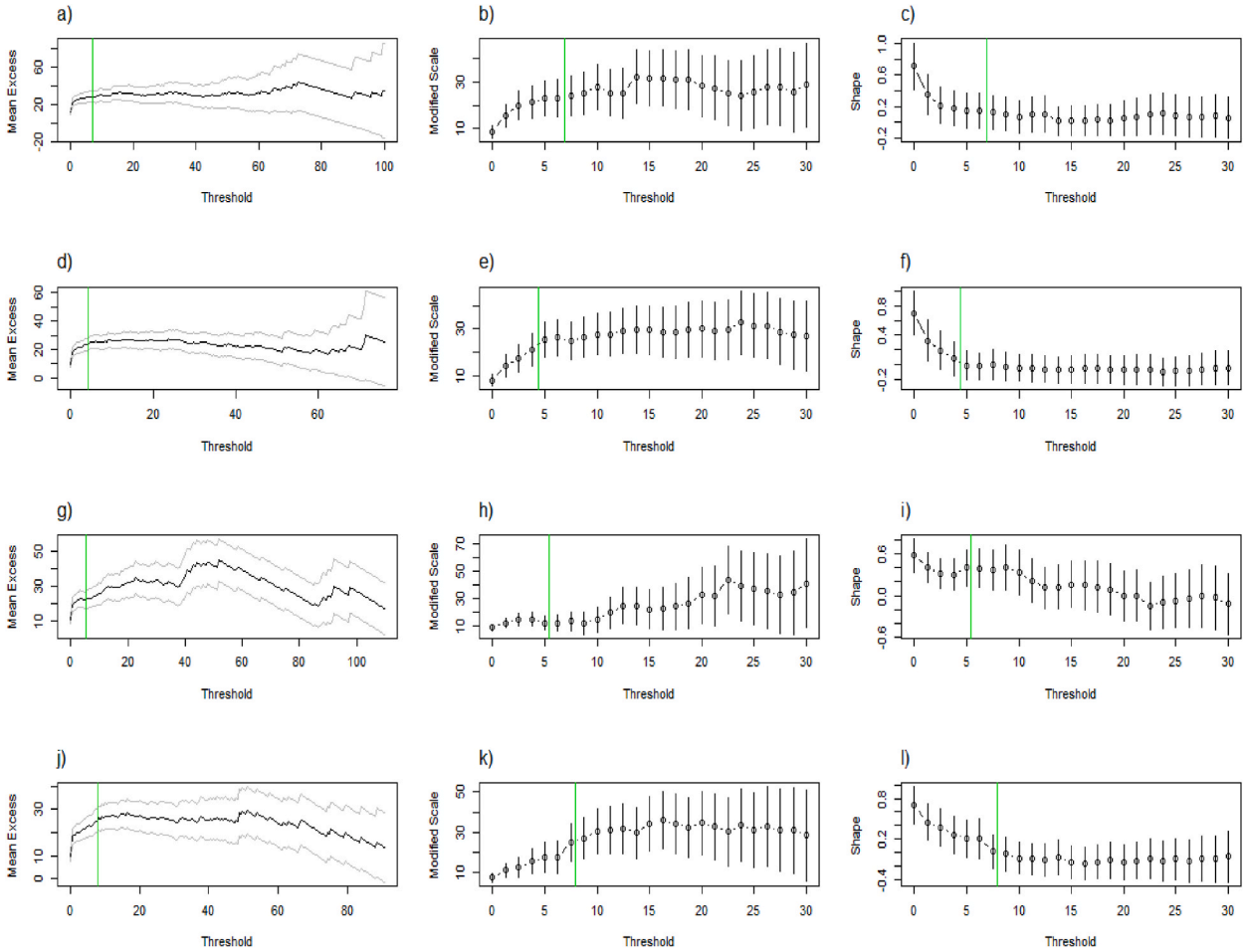


**Fig. 7.** Mean Residual Life (MRL) plots (figs. a-*d*-g-j) and Model-Based Check (MBC) plots (figs. b–c, e-f, h-i, k-l) for Douala city rainfall data for the years 2011 (a-b-c); 2012(d-e-f); 2013 (g-h-i) and 2014 (j-k-l). The same interpretations are made for the MRL and MBC plots as in Fig. 4.

(2) If the upper limit of return periods is an integer, then the upper limit of number of return days corresponds to the upper limit of return periods. Otherwise, the upper limit of number of return days corresponds to the round up to the integer of upper limit of return period confidence interval.

For example: if the confidence interval for the return period is [58.9, 60.01], then the confidence interval for the number of return days is [58, 61].

(ii) We consider the list of extreme value dates established in section 2.3.3.1.
(iii) We then add to these dates the numbers found at the lower (upper) limits of the confidence intervals for the number of return days to find the lower (upper) limits of the confidence intervals for the return dates, taking into account leap years, where February has 29 days; i.e., the confidence interval for the return date of precipitation recorded on February 20, 2016 for the confidence interval for the number of return days of [9,15] was [February 29, 2016, March 14, 2016].

## 3. Results and discussions

### 3.1. Variability of rainfall in douala city

Fig. 3 shows the daily rainfall distribution (Fig. 3a), as well as a breakdown by year over (Fig. 3b) and daily mean rainfall amount in each month (Fig. 3c) of Douala city for the period from 2011 to 2021. Fig. 3 a presents a maximum of about 345.4 mm was obtained on the June 22, 2016. This date remains historic for the people of Douala city. It corresponds to a date of memorable flood and consequences in this city. Several newspapers report (http://ct2015.cameroontribune.cm/index.php?option=com_content&view=article&id=97225%3A2016-06-27-08-4535&catid=3%3Adossier-de la; https://africtelegraph.com/cameroucapitale-economique-leau/; https://matango.mondoblog.org/th%C3%A8me/inondation/) also noted the damages caused by the

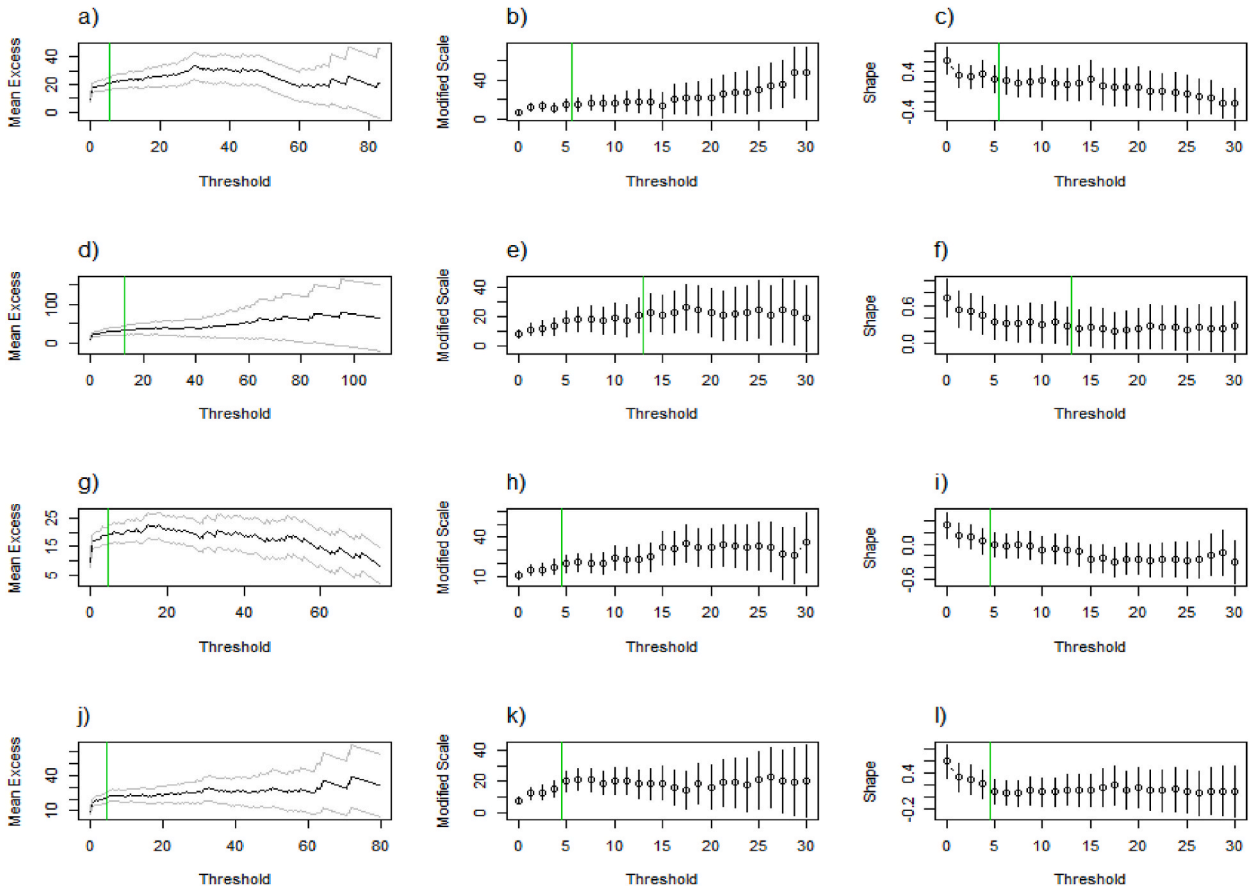


**Fig. 8.** The same plots as Fig. 7 but with data from 2015 (figs. a-b-c); 2016 (figs. d-e-f); 2017 (figs. g-h-i) and 2018 (figs. j-k-l).

floods of June 22, 2016 in Douala. Fig. 3 b displays the precipitations peaks in each year of the distribution. These peaks of heavy rainfall also caused several floods in Douala city. For example, the maximum rain (83 mm) of 19 June 2015was at the origin of the floods that caused several damages and the death of two people (https://www.cameroon-info.net/article/cameroun-inondations-geantes-a-douala-ce-samedi-20-juin-2015-244608.html). Fig. 3 c presents the mean daily rainfalls for the months of January to December on the study period (2011–2021). This figure shows that the daily precipitation mean is low for December-January-February (DJF) period. This period gives a frequency of rainy days less than five days per month and is considered as the great dry season according to the study of the weather conditions for aviation safety in Douala [42]. These rains sometimes cause the floods in certain localities of Douala city. This was the case of the rains of January 15, 2013, when 13.4 mm of rainfall was recorded, causing floods in the marshy shallows of neighborhoods such as Ngangue, Makepe Missoke, Mabanda and Cité des Palmiers [7]. In March-April-May (MAM) period corresponding to the small rainy season, the mean rainfalls exceed 5 mm per day. After [68], this period is important for agriculture as a preparatory phase before the great rainy season of June-July-August-September (JJAS). In JJAS period which is the great rainy season, the maximum precipitations values reach more than 15 mm per day in mean. This period corresponds to the monsoon season in Douala and it has the highest frequency of rainy days, exceeding 20 days/month [42]. Therefore, the floods and their consequences are more important in this season. The majority of the return dates which will be determined, will be the dates of the different month of the JJAS period. Lastly, October–November (ON) period is an intermediate season between the great rainy season in JJAS and the great dry season in DJF. It corresponds to a rapid decrease of the precipitation and the mean rains are above 6 mm/days.

### *3.2. General parato distribution (GPD) model fitting and goodness of fit to rainfall data for douala city*

#### *3.2.1. General Pareto Distribution (GPD) model fitting and threshold selection*

Good adaptation of the GPD model requires better threshold selection. The graphical approach is therefore shown in Fig. 4 to enable the correct choice of this threshold. This figure shows the Mean Residual Life (MRL) and model-based check (MBC) curves for daily rainfall of Douala city over the period 2011–2021. The MRL technique gives a linear approximation for threshold values, while the MBC technique is based on the stability of the GPD model modified scale and shape parameters relative to the threshold, after fitting the inferred distribution over a range of different thresholds. An analysis of the MRL plot (Fig. 4a) for rainfall data gives the

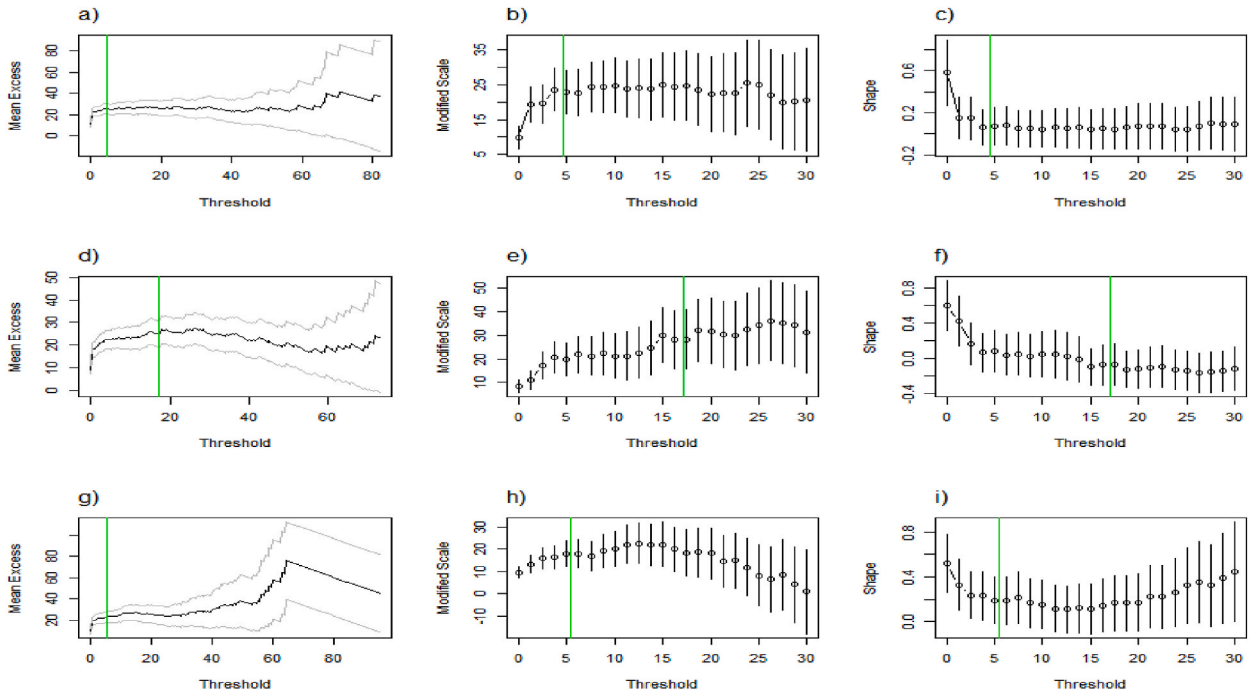


**Fig. 9.** The same plots as Fig. 7 but with data from 2019 (figs. a-b-c); 2020 (figs. d-e-f) and 2021 (figs. g-h-i).

10–30 mm (range separated by two red lines) ranges as threshold values that make the inferred distribution approximately linear. Furthermore, using the MBC plots (Fig. 4 b-c) of GPDs fitted to the ranges of the MRL technique, a specific threshold value chosen is 12.5 mm (green value on the plots) as it is specifically observable in the threshold value showing the stability of the modified scale and shape parameters of the GPD model with respect to thresholds for each variable. The threshold here represents a value beyond which floods are produced in the city. A value of 13.4 mm had already caused floods in Douala [7]. Therefore, a rainfall amount of about 12.5 mm is a good choice, because precipitation data exceeding this value is a threshold violation.

The approach by the threshold selection algorithm method confirms our choice. Indeed, the determination of the threshold by this technique also gives a threshold value u equal to 12.5 mm. This threshold value gives a number of extremes, nextreme equal to 875

Once the best threshold selection is made, the inference of the model parameters will be performed by the Maximum Likelihood Method (MLE).

### *3.2.2. Quality of fit: diagnosing the GPD model using the maximum likelihood method (MLE) method*

Fig. 5 shows the diagnostic graphs of the Generalized Pareto Distribution (GPD) fitted to rainfall data for the city of Douala over the period 2011–2021 to establish the pertinence of the choice of threshold. The GPD model fit test performed using these graphs, in which empirical data are compared with aspects of the inferred GPD model, generates two main results.

(1) The Probability plots and quantile-quantile diagrams give an ensemble of points respectively linear (Fig. 5a) and quasi-linear (Fig. 5.b).
(2) The histogram is well followed by the adjusted density functions (Fig. 5c).

These results reinforce the relevance of the chosen threshold and justify the good compatibility between the GPD and precipitation extremes above the selected threshold.

Estimates of the GPD model parameters (scale, shape) using the MLE method are presented in Table 2, with 95 % Confidence Intervals (CIs) and standard estimation errors. The value obtained for the shape parameter ($\xi$) is $0.0947 \pm 0.036$ ($\xi > -0.5$) for a CI of [0.005, 0.153]. The positivity of this parameter shows that the distribution is of the heavy-tailed Pareto type [59]. The estimates of Return Periods (RPs) and Return Levels (RLs) imply systematic knowledge of the parameters of the adjusted GPD, hence the importance of the estimation of these parameters.

### *3.2.3. Return periods (RPs), return dates (RDs) and return levels (RLs) for the extreme's precipitations in douala city*

Fig. 6 presents the curve of RLs (mm) as a function of RPs (day) (Fig. 6 a) and RPs (day) relative to RLs (mm) (Fig. 6b) of the daily cumulations of precipitation in Douala city over the period from 2011 to 2021 (continue lines of Fig. 6 a-b). These curves are surrounded by dotted lines, which represent the 95 % CIs calculated using the Delta method.

These figures show that RLs functions and RPs functions increase in relation to each other. Both functions (RPs and RLs) are

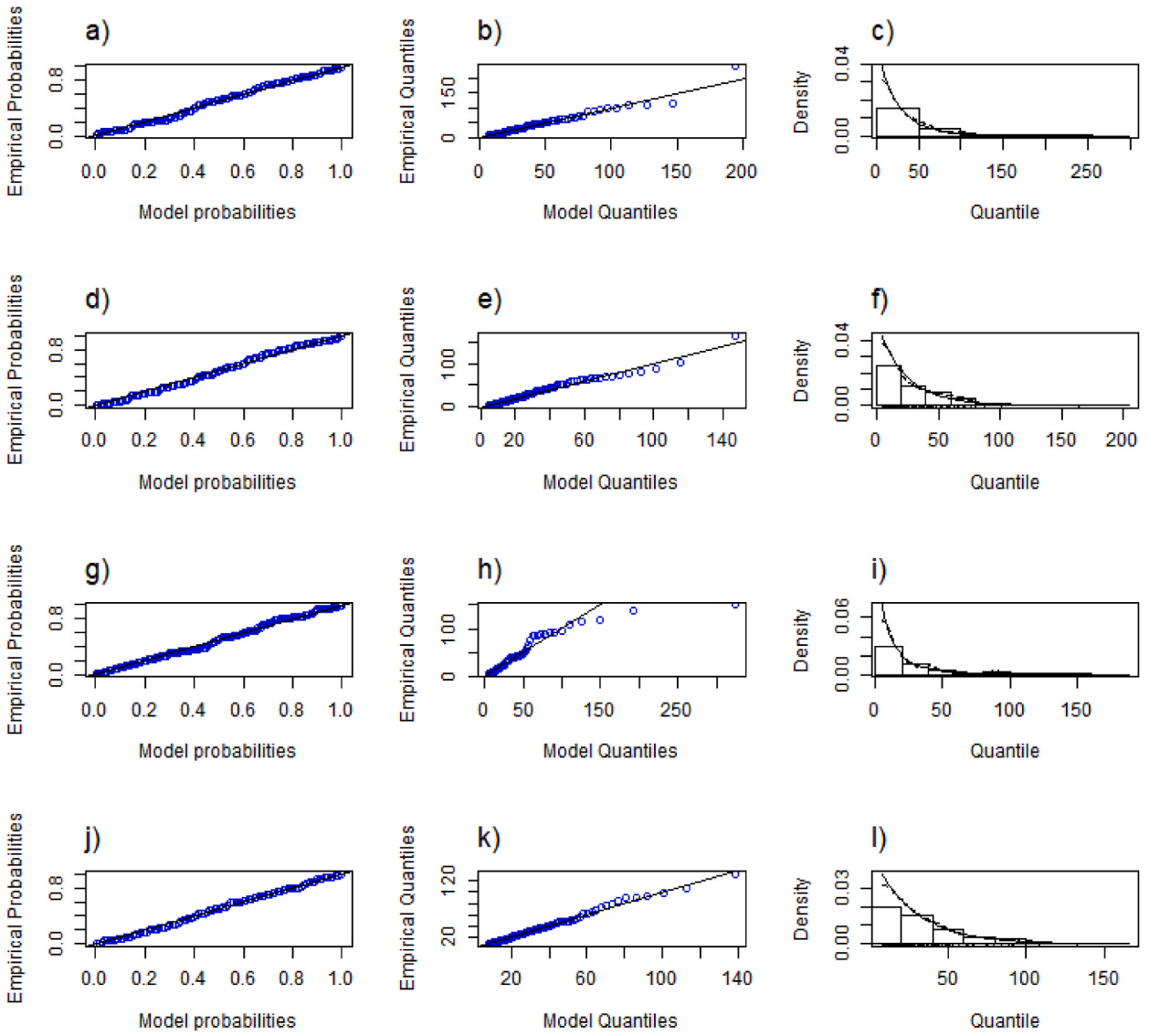


**Fig. 10.** Diagnostic plots for the generalized Pareto distribution (GPD) fitted to 2011 rainfall data (Fig a-b-c); 2012 (Fig. d-e-f); 2013 (Fig g-h-i) and 2014 (Fig. j-k-l): this plot shows probability plots (Fig. a-*d*-g-j); quantile-quantile plots (Fig. b-e-h-k); and histograms of the fitted data and density functions (Fig. c-f-i-l).

reciprocal. In addition, the two graphs present CIs that enlarge considerably with the increase in RP and RL. From another point of view, the curve on Fig. 6 a also reinforces the good match between the choice of threshold and the fit of the model, because the empirical values follow the model adjusted by the GPD.

Table 3 gives the results of the estimation of some return periods (chosen arbitrarily), as well as the associated return levels. This table contains also the Confidence Intervals (CIs) for Return Periods (RPs) and Return Levels (RLs). It shows that for rains less than 140 mm, their RPs are lower than one year. In general, these rains are returned in the same year as their extreme values. The CIs of their RPs and RLs are less spaced around their values. For rains in excess of 140 mm, return periods surpass one year. The CIs for their RPs and RLs are more spaced around their values.

Table 4 presents the RPs in relation to the maximum precipitation over each year, the dates of the maximum precipitations, the extreme precipitation and the estimated dates of the return of extreme rainfall. It also presents the CIs of the RPs, RLs with the dates of the extreme rainfalls.

This table shows that the maximum value of our sample (345.4 mm) has a return period of 45187 days. Corresponding to 123 years 292 days later. The return date for this value is March 10, 2141 and its CI at 95 % is [September 01, 2025,June 10, 2217]. Therefore, such a level of precipitation can return between 2025 and 2217.

In the following, the return times of rainfall that can cause floods in Douala city will be studied. Therefore, the peak rainfalls

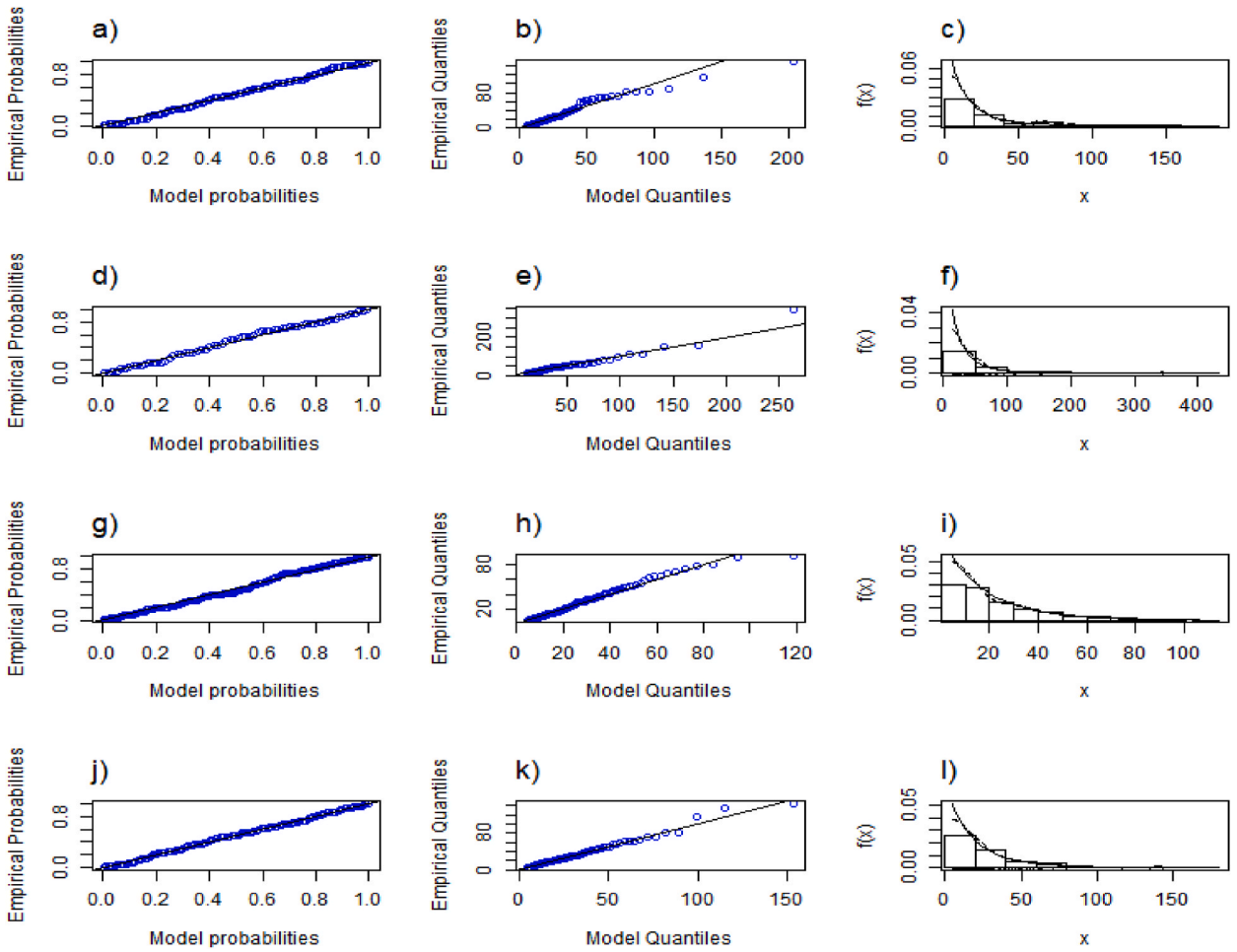


**Fig. 11.** The same plots as in Fig. 10 with data from 2015 (Fig a-b-c); 2016 (Fig d-e-f); 2017 (Fig. g-h-i) and 2018 (Fig j-k-l).

causing floods are distributed over each year of the data distributions. An application of the GPD model to daily precipitation per year on the period 2011–2021 is also required.

### 3.3. Prediction of future flood dates in douala

#### 3.3.1. Adjustment and quality of adjustment of the GPD model to daily precipitation per year over the period 2011–2021

Figs. 7–9 are plotted in order to make a good choice of threshold for the daily distributions of precipitation year per year, over the period from 2011 to 2021. They are obtained by applying the same principles of section 3.2.1 on MRL analysis (Fig. 7a-*d*-g-j; Fig. 8a-*d*-g-j and Fig. 9a-*d*-g) and MBC (Fig. 7b and c, 7e-f, 7h-i, 7k-l; Fig. 8b and c, 8e-f, 8h-i, 8k-l and Fig. 9 b-c, 9e-f, 9h-i).

Considering also the threshold selection algorithm, it can be seen that the thresholds u (mm) used are: 6.916935, 4.37936, 5.4, 7.9, 5.5, 13.0, 4.5, 4.461988, 4.573753 , 17.1 and 5.4 mm for 2011 to 2021, respectively. The green lines are illustrated to show the thresholds on the different tracks.

Figs. 10–12 verify the adequacy between the thresholds and the adjusted GPD models. Examination of these figures shows that empirical probability functions (Fig. 10 a, d, g, j; Fig. 11 a, d, g, j; Fig. 12 a, d, g) and quantile-quantile functions (Fig. 10 b, e, h, k; Fig. 11b–e, h, k and Fig. 12 b, e, h) are quasi-linear. It is important to note that the density functions are in agreement with different histograms (Fig. 10 c, f, i, l; Fig. 11 c, f, i, l and Fig. 12 c, f, i). These graphs give the diagnoses of the generalized Pareto distribution function applied to the 2011 rainfall data (Fig. 10 a-c); 2012 (Fig. 10 d-f); 2013 (Fig. 10 g-h); 2014 (Fig. 10 j-k); 2015 (Fig. 11 a-c); 2016 (Fig. 11 d-f); 2017 (Fig. 11 g-h); 2018 (Fig. 11 j-k); 2019 (Fig. 12 a-c); 2020 (Fig. 12 d-f); 2021 (Fig. 12 g-h). These figures thus prove the pertinence of thresholds selected above on precipitation data per year for the study period.

#### 3.3.2. Return dates of extreme precipitation in each year that can cause floods in douala city

Fig. 13 a-k presents extreme precipitation return levels, resulting from daily rainfall year per year over the period from 2011 to 2021, represented by Fig. 13 a-k. These figures show a growth of RLs as a function of RPs. 95 % CIs are also represented (dotted lines).

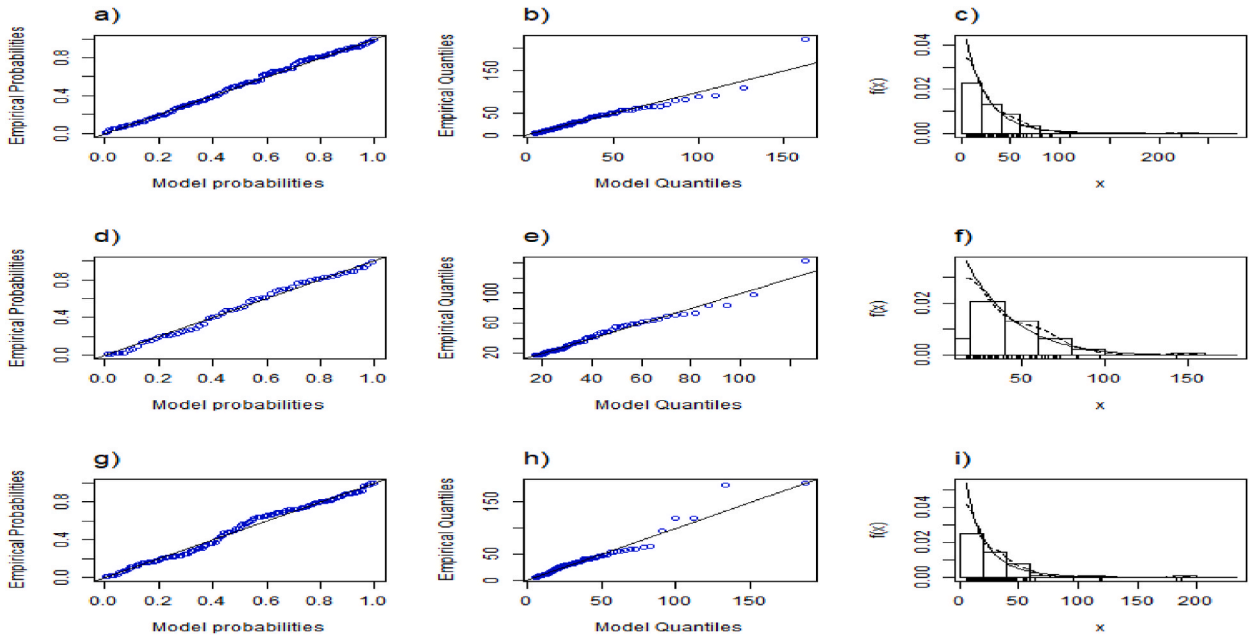


**Fig. 12.** The same plots as in Fig. 10 with data from 2019 (fig. a, b, c); 2020 fig. d, e, f) and 2021(fig. g, h,i).

We can see that the CIs enlarge for elevated RP and RL values.

Table 5 in appendix A, present the dates of probable floods in Douala city over the period 2011–2021, including the rainfall levels (in mm) received during these probable floods, the estimates of the RPs (in day) and the return dates of future floods as well as the 95 % CIs.

An analysis of this table shows that in a future projection, a few points of extreme precipitations can be observed during the well months great dry season (December, January, February). The return dates of extreme rainfalls leading to major floods remain the dates of the great rainy season (June-July-August-September period).

### *3.4. Discussion*

The results obtained for estimated Return Dates (RDs) are very interesting and in agreement with passed dates of floods in Douala, given on table 6 in appendix B. Furthermore, the return level found are greater than the threshold of floods in the city. Indeed, a quick look at the return dates found, shows that floods appear during the June-July-August-September (JJAS) period corresponding to the great rainy season as mentioned in Figs. 2 and 3 c. These similarities between (i) our return dates and the dates of floods recorded on table 6 in appendix B, (ii) our return levels in the confidence intervals (CIs) and the threshold of flood found in Douala, can be considered as the validation of our methods in this work. Therefore, the projection made for future years can be considered as reality and could help for different uses.

We have determined the confidence intervals of return dates (RDs) and return levels (RLs). It should be noted that the RDs and RLs found are inside their confidence intervals. These CIs were obtained at 95 % using Delta method to find estimated dates and level close the real values. For example, the rain of April 16, 2013 (150 mm), has a return date of August 12, 2014. The confidence intervals of return level and return date were [131.66, 168.46] and [June 23, 2014, January 02, 2015], respectively. A precipitation of 132.2 mm was recorded on August 11, 2014. The real date and the estimates date are offbeat of one day. Booth dates are in the confidence interval of return dates. So, the real value 132.2 mm is in the CI of the return levels and was recorded one day before the estimated return date.

Thus, the confidence intervals of return dates and return levels most be short and contain real and estimates values. So, the early warning will be closer to the effective dates of flood.

## 4. Conclusion

The aim of this work was to determine Return Periods (RPs), Return Levels (RLs), Return Dates (RDs) and their Confidence Intervals (CIs) of extreme rainfall in Douala city. We have used the daily rainfall data for the Douala weather station acquired from the data of the synoptic report found on http://www.ogimet.com/guia.phtml.en, for the period 2011 to 2021. The univariate and stationary Peak-Over-Threshold (POT) have been applied to these data to estimate RPs and RLs, through Generalized Pareto Distribution (GPD) fitted to the values depending on the selected thresholds. These selected thresholds were made using three methods: (i) Mean Residual Life (MRL), (ii) Model-Based Check (MBC) and (iii) automatic threshold selection algorithm. The confidence intervals were determined by means of the Delta method.

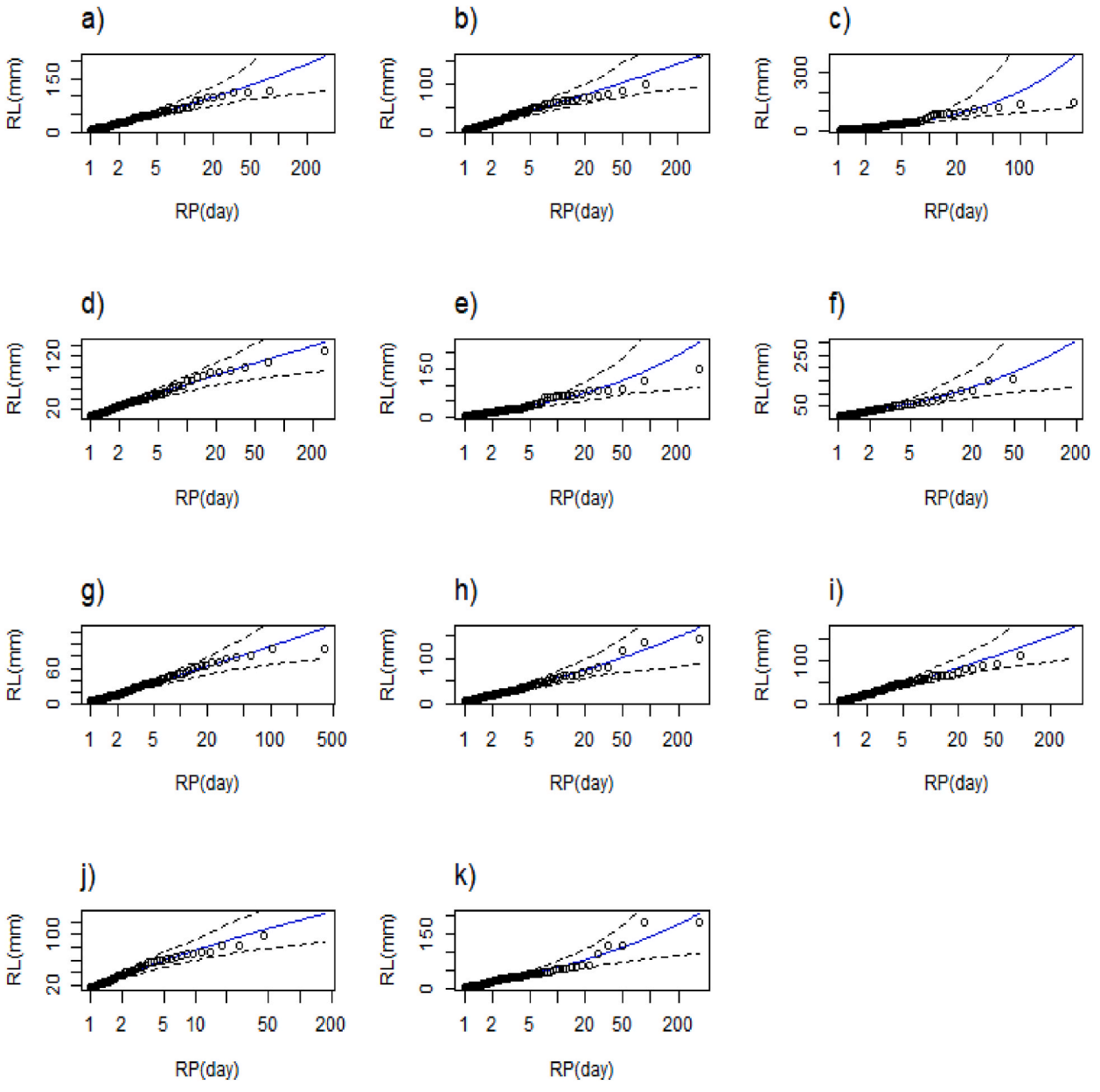


**Fig. 13.** Plots of the return levels of extreme daily rainfall of the 2011-21 rainfall data per year, represented by the respective plots of figs (a–k) in Douala, calculated from the GPD distribution (black line curve) surrounded by the 95 % confidence intervals (dashed lines), calculated by the Delta method.

The results obtained show that, based on daily rainfalls from 2011 to 2021, four seasons were detected in Douala city: December-January-February (DJF), March-April-May (MAM), June-July-August-September (JJAS) and October–November (ON). DJF period is the great dry season. The frequency of rainy days is low (five days by month). In general, the floods and their consequences are not important during this period. However, the rains of amount greater than 12.5 mm were found causing floods in marshy neighbourhoods of Douala city. MAM period corresponds to the small rainy season. The frequency of floods and their consequences begin to increase in this season. MAM is followed by the greatest rainy season of JJAS. In JJAS period, Douala city records the greatest precipitations values and therefore, very devastating floods. We found the memorable flood of June 22, 2016 with the daily rainfall value 345.4 mm. The last season corresponding to ON period is intermediate between the great rainy season of JJAS and the great dry season of DJF, and characterized by a rapid decrease of the rainfalls and floods. Finally, the heavy floods in Douala city occurred during JJAS season with highest rainfall amounts.

The best General Pareto Distribution (GPD) model was then applied to the daily rainfall data. The diagnostic diagrams of the GPD model by the Maximum Likelihood Method (MLE) showed a good match of the model to the selected threshold exceedance. These

diagrams showed the relevance of the chosen thresholds. In this logic, the GPD model was the most appropriate to make a study on the extreme daily rainfall in Douala city.

Estimates of RPs and RDs of extreme precipitation over the period 2011–2021 indicate that maximum precipitation returns every 45187 days (345.4 mm). It is therefore important to note that such a value must arrive after 123 years 292 days corresponding to March 10, 2141.

Estimates of RPs and RDs of precipitations that caused floods in the Douala city present very good results compared to the dates of observed floods mainly during the great rainy season (June, July, August and September). These months are indicated as the months with the most intense floods in the city.

We have also determined the Confidence Intervals (CIs) of the RPs and RDs. These CIs allow to know the maximum and minimum values surrounding the RPs and RDs. We note that, all the RPs and RDs found belong to these CIs. For example, the rainfall of 150 mm, recorded on April 16, 2013 have a return date scheduled the August 12, 2014 whose CI of RLs is [131.6553, 168.4553] and its CI of return date is [June 23, 2014, January 02, 2015]. However, a value of 132.2 mm that is in the interval [131.6553, 168.4553] has been recorded on the August 11, 2014 that is in the interval [June 23, 2014, January 02, 2015]. The dates of the flood recorded in 2014 and those projected by the estimates are very close. This shows the relevance of the determined estimates.

Finally, this work has allowed to determine the Return Periods (RPs) and Return Levels (RLs) with their Confidence Intervals (CIs) and has proposed a method to determine the Return Dates (RDs) with their CIs of the extreme rainfall. This estimation of RDs could help to early warning of the floods in Douala city. The method used to determine RPs, RDs, RLs and their CIs can be applied to any other city in the world and for other climatic parameters.

Here, we have used the daily data to determine the RDs of the extremes, but if the hourly data are available, this method can be also applied. So, we can determine the return dates and the return hours of the dates for these extreme rainfalls.

## Data availability statement

We used daily precipitations (2011–2021) acquired by synoptic reports data for Douala meteorological station (World Meteorological Organization-WMO-index of 64,910). The Ogimet weather information service stores database for all meteorological services around the whole world. It is based on WMO and the international aviation organization (ICAO) station indices. It is the case of Douala meteorological station. The daily means are based directly on climate reports (FM 71-XI), usually available during the first 10 days of the next month (see http://www.ogimet.com/guia.phtml.en for some details).

## CRediT authorship contribution statement

**Calvin Padji:** Writing – review & editing, Writing – original draft, Visualization, Validation, Software, Methodology, Data curation, Conceptualization. **Cyrille Meukaleuni:** Supervision, Project administration. **Cyrille Mezoue Adiang:** Project administration. **Daniel Bongue:** Project administration. **David Monkam:** Writing – review & editing, Writing – original draft, Supervision.

## Declaration of competing interest

The authors declare that they have no known competing financial interests or personal relationships that could have appeared to influence the work reported in this paper.

## Acknowledgement

The authors thank the Ogimet organization for their daily precipitations data of the Douala station. They thank also the local newspapers for the publication of the flood dates.

## Appendix A

**Table 5**
Dates of the floods recorded in the city of Douala in 2011–21, their level of rainfall (mm), estimates of return periods (Days) of these floods, as well as the estimated dates of the rains causing the next floods. As well as 95 % confidence intervals.

| Dates of the extremes Rainfall | Rainfall levels(mm). | RP of rains (day). | Return dates of rainfall levels causing floods. | 95 % confidence interval for RLs |
|---|---|---|---|---|
| July 02, 2011 | 99.5 | 71 | September 11, 2011 | [75.68, 124.11] |
| July 21, 2011 | 109.4 | 93 | October 21, 2011 | [81.07, 138.25] |
| July 26, 2011 | 115.3 | 109 | November 12, 2011 | [84.03, 147.04] |
| July 31, 2011 | 90.1 | 54 | September 23, 2011 | [69.818, 110.74] |
| August 04, 2011 | 64.7 | 25 | September 29, 2011 | [51.62, 77.73] |
| August 18, 2011 | 100.1 | 72 | October 28, 2011 | [75.97, 124.82] |
| August 21, 2011 | 67.2 | 28 | September 18, 2011 | [54.41, 82.21] |

(*continued on next page*)

**Table 5** (*continued*)

| Dates of the extremes Rainfall | Rainfall levels(mm). | RP of rains (day). | Return dates of rainfall levels causing floods. | 95 % confidence interval for RLs |
|---|---|---|---|---|
| August 28, 2011 | 58.3 | 21 | September 19, 2011 | [47.28, 71.04] |
| September 04, 2011 | 72.2 | 32 | October 06, 2011 | [57.67, 87.65] |
| September 07, 2011 | 70.5 | 30 | October 07, 2011 | [56.1, 85] |
| September 13, 2011 | 238.6 | 1844 | April 17, 2017 | [104.36, 372.9] |
| October 16, 2012 | 110.4 | 95 | January 03, 2012 | [81.47, 139.41] |
| June 27, 2012 | 163.3 | 1265 | June 18, 2015 | [92.02, 234.62] |
| August 04, 2012 | 62.9 | 33 | September 07, 2012 | [50.61, 74.13] |
| April 07, 2013 | 109.7 | 80 | June 26, 2013 | [66.98, 152.94] |
| April 16, 2013 | 150 | 147 | September 10, 2013 | [77.61, 223.27] |
| July 03, 2013 | 139.7 | 127 | August 07, 2013 | [75.10, 202.19] |
| July 10, 2013 | 91.4 | 57 | September 04, 2013 | [60.01, 123.13] |
| October 07, 2013 | 97.2 | 64 | December 09, 2013 | [62.44, 132.67] |
| October 19, 2013 | 89.7 | 55 | November 24, 2013 | [59.25, 120.32] |
| November 14, 2013 | 116.2 | 89 | February 11, 2014 | [69.05, 163.58] |
| April 04, 2014 | 107.9 | 201 | October 22, 2014 | [80.10, 134.910] |
| May 13, 2014 | 90.8 | 99 | August 20, 2014 | [71.53, 109.10] |
| August 11, 2014 | 132.2 | 559 | February 21, 2014 | [89.88, 174.53] |
| September 24, 2014 | 91.7 | 103 | January 05, 2015 | [72.14, 111.33] |
| June 03, 2015 | 114.5 | 157 | November 07, 2015 | [67.78, 161.33] |
| June 19, 2015 | 83 | 74 | September 02, 2015 | [56.85, 109.65] |
| August 27, 2015 | 82.7 | 73 | November 07, 2015 | [56.63, 108.87] |
| October 19, 2015 | 148.6 | 306 | August 20, 2016 | [73.97, 223.21] |
| May 13, 2016 | 94.7 | 61 | July 12, 2016 | [64.43, 124.66] |
| June 22, 2016 | 345.4 | 1584 | October 24, 2019 | [41.78, 648.89] |
| July 15, 2016 | 112.2 | 87 | October 10, 2016 | [41.78, 648.88] |
| August 06, 2016 | 153.5 | 179 | February 02, 2017 | [83.54, 223.51] |
| September 05, 2016 | 109.4 | 83 | November 27, 2016 | [71.25, 148.00] |
| May 24, 2017 | 91.4 | 205 | December 15, 2017 | [67.48, 115.33] |
| July 03, 2017 | 75.2 | 95 | October 06, 2017 | [59.19, 91.39] |
| July 24, 2017 | 79.2 | 115 | November 16, 2017 | [61.44, 97.08] |
| August 13, 2017 | 91.1 | 203 | March 04, 2018 | [67.39, 115.01] |
| September 07, 2017 | 81 | 126 | January 11, 2018 | [62.47, 99.86] |
| June 18, 2018 | 62.5 | 44 | August 02, 2018 | [50.69, 79.06] |
| July 18, 2018 | 135.2 | 439 | September 30, 2019 | [80.01, 190.46] |
| July 25, 2018 | 144.2 | 566 | February 11, 2020 | [81.43, 207.08] |
| August 20, 2018 | 79.3 | 75 | November 03, 2018 | [59.69, 99.35] |
| August 30, 2018 | 116.1 | 250 | May 07, 2019 | [75.38, 157.01] |
| October 12, 2018 | 80 | 77 | December 28, 2018 | [60.10, 100.43] |
| June 24, 2019 | 90.8 | 78 | September 10, 2019 | [70.09, 111.73] |
| July 25, 2019 | 222.2 | 3793 | October 12, 2028 | [95.16, 349.25] |
| July 27, 2019 | 109.3 | 144 | December 18, 2019 | [79.8, 138.84] |
| August 19, 2019 | 70.5 | 38 | September 26, 2019 | [56.56, 84.06] |
| July 03, 2020 | 62.6 | 35 | August 07, 2020 | [50.49, 74.37] |
| July 23, 2020 | 83.2 | 87 | October 18, 2020 | [67.08, 99.4] |
| August 21, 2020 | 142.7 | 1911 | October 15, 2025 | [89.67, 195.74] |
| September 15, 2020 | 97.5 | 170 | May 04, 2021 | [76.5, 118.55] |
| October 16, 2020 | 70.3 | 49 | December 04, 2020 | [57.04, 83.58] |
| August 11, 2021 | 186.2 | 720 | August 01, 2023 | [85.9, 286.51] |
| August 25, 2021 | 59.8 | 31 | September 25, 2021 | [46.29, 72.61] |
| September 01, 2021 | 183.1 | 680 | July 12, 2023 | [85.88, 280.39] |
| September 02, 2021 | 118.5 | 171 | February 20, 2022 | [75.7, 161.42] |
| September 15, 2021 | 95.1 | 93 | December 17, 2021 | [66.71, 123.64] |
| September 20, 2021 | 58.7 | 30 | October 20, 2021 | [45.63, 71.37] |
| October 21, 2021 | 119.2 | 174 | April 13, 2022 | [75.92, 162.62] |

## Appendix B

**Table 6**
Dates of floods and website to obtain these dates for period 2011 to 2021 in the Douala city.

| Dates of floods | Website of flood dates |
|---|---|
| June 21, 2011 | [7]/http://hdl.handle.net/2268.2/5575 |
| August 18, 2011 | |
| September 13, 2011 | |
| June 27, 2012 | |
| July 03, 2013 | |
| August 11, 2014 | |
| June 19, 2015 | https://www.camer.be/mobile/43778/11:1/cameroun-habitat-douala-panse-encore-les-plaies-des-inondations-cameroon.html |
| June 21, 2015 | https://actucameroun.com/2016/06/24/cameroun-inondation-grosses-pluies-et-consequences-a-douala/ |
| July 3, 2015 | https://reliefweb.int/report/cameroon/les-camerounais-frapp-s-par-les-inondations-urbaines |
| June 22, 2016 | https://africtelegraph.com/cameroucapitale-economique-leau/ |
| September 07, 2017 | https://actucameroun.com/2017/09/16/cameroun-inondations-populations-de-ville-de-douala-desarroi-apres-trois-jours-de-pluie-cesse/ |
| July 25, 2018 | https://yusiip.cm/actualite_presentation.php?actualite=76 |
| July 25, 2019 | https://philieradar.com/inondation-a-douala-les-autorites-administratives-sont-elles-responsables/ |
| July 03, 2020 | https://actucameroun.com/2020/07/06/cameroun-les-inondations-sont-de-retour-a-douala/ |
| 13–14 July 2020 | https://actucameroun.com/2020/07/15/changement-climatique-douala-sous-les-eaux/ |
| July 23, 2020 | https://actucameroun.com/2020/07/24/cameroun-un-enfant-de-4-ans-emporte-par-les-eaux-a-douala/ |
| 19–21 August 2020 | https://www.237online.com/cameroun-des-inondations-aux-allures-de-deluge-a-douala/ |
| August 21, 2020 | http://www.cameroon-info.net/article/cameroun-intemperies-les-inondations-sont-de-retour-a-douala-380916.html%20, |
| September 15, 2020 | https://actucameroun.com/2020/09/20/douala-pourquoi-le-cauchemar-des-inondations-persiste/ |
| August 11, 2021 | https://www.cameroun24.net/blog/affobo/?pg=actu&ppg=1&pp=1&id=57621 |
| September 01, 2021 | https://www.infoscameroon.com/tag/inondation-douala/ |
| September 02, 2021 | https://www.camerounweb.com/CameroonHomePage/NewsArchive/Inondation-la-ville-de-Douala-en-voie-de-disparition-616852 |
| September 15, 2021 | https://www.cameroon-tribune.cm/article.html/42400/fr.html/douala-nouvelles-pluies-nouveaux |
| September 20, 2021 | https://www.cameroon-tribune.cm/article.html/42400/fr.html/douala-nouvelles-pluies-nouveaux |

## References


[1] J.C. Bertoni, Inondations urbaines en Amérique Latine: réflexions sur le rôle des facteurs de risque, Front. flood Res. 305 (2006) 123–141.
[2] T. De Groeve, Z. Kugler, G.R. Brakenridge, Near real time flood alerting for the global disaster alert and coordination system, Proc. ISCRAM (2007) 33–39.
[3] D. Paprotny, A. Sebastian, O. Morales-Nápoles, S.N. Jonkman, Trends in flood losses in Europe over the past 150 years, Nat. Commun. 9 (1) (2018) 1985.
[4] H.-J. Scarwell, R. Laganier, Risque d'inondation et aménagement durable des territoires, vol. 916, Presses Univ. Septentrion, 2004.
[5] S.I. Khan, et al., Remote sensing applications satellite remote sensing and hydrologic modeling for flood inundation mapping in lake victoria basin: implications for hydrologic prediction in ungauged basins, IEEE Trans. Geosci. Rem. Sens. 49 (1) (2011) 85.
[6] L. Bruckmann, A. Amanejieu, M.O.Z. Moffo, P. Ozer, Analyse géohistorique de l'évolution spatio-temporelle du risque d'inondation et de sa gestion dans la zone urbaine de Douala (Cameroun), Physio-Géo. Géographie Phys. Environ. 13 (2019) 91–113.
[7] A. Amanejieu, Travail de fin d'études:" ANALYSE TEMPORELLE DE LA REPRESENTATIONDU RISQUE D'INONDATION DE 1980 A 2018 A DOUALA-CAMEROUN, 2018.
[8] Climate Impacts on African Hydropower".
[9] K.E.Y. Messages, Climate Risks in Africa, 2022.
[10] M.B.D. Ahouangan, Y.C. Hountondji, A. Thiry, F. De Longueville, B. Djaby, P. Et Ozer, Adaptation et résilience des populations rurales face aux catastrophes naturelles en Afrique subsaharienne, Cas des inondations (2010) 265–278.
[11] H. Issaka, Mise en carte et gestion territoriale des risques en milieu urbain sahélien à travers l'exemple de Niamey (Niger), 2010. Strasbourg.
[12] OCHA, Afrique de l ' Ouest • Inondations 2009, 2009.
[13] dfomission.pdf".
[14] A. Amanejieu, R.A. Feumba, R. Ngoufo, P. Ozer, Vulnérabilité aux inondations dans le contexte des changements climatiques à New-Bell Ngangue, un quartier planifié de la ville de Douala, Cameroun, in: Multidisciplinary Workshop Disasters and Resilience in the 21st Century, 2017.
[15] E. Tonye, CARTOGRAPHY OF FLOOD PRONE AREAS AND ASSESSMENT OF FLOODING HOUSING IN DOUALA (CAMEROON), 2013.
[16] C. Roméo, Etude des Evénements Extrêmes: cas des Températures et Précipitations à Douala, 2012.
[17] Y. Tramblay, W. Badi, F. Driouech, S. El Adlouni, L. Neppel, E. Servat, Climate change impacts on extreme precipitation in Morocco, Global Planet. Change 82 (2012) 104–114.
[18] Z. Li, Z. Li, W. Zhao, Y. Wang, Probability modeling of precipitation extremes over two river basins in northwest of China, Adv. Meteorol. 2015 (2015).
[19] Y.A. Seo, Y. Lee, J. Park, M. Kim, C. Cho, H. Baek, Assessing changes in observed and future projected precipitation extremes in South Korea, Int. J. Climatol. 35 (6) (2015) 1069–1078.
[20] T.M. Vu, A.K. Mishra, Nonstationary frequency analysis of the recent extreme precipitation events in the United States, J. Hydrol. 575 (2019) 999–1010.
[21] Z. Yuan, Z. Yang, D. Yan, J. Yin, Historical changes and future projection of extreme precipitation in China, Theor. Appl. Climatol. 127 (2017) 393–407.
[22] M.A. Sarr, O. Seidou, Y. Tramblay, S. El Adlouni, Comparison of downscaling methods for mean and extreme precipitation in Senegal, J. Hydrol. Reg. Stud. 4 (2015) 369–385.
[23] M.A. Osei, et al., Estimation of the return periods of maxima rainfall and floods at the Pra River Catchment, Ghana, West Africa using the Gumbel extreme value theory, Heliyon 7 (5) (2021) e06980.
[24] T.A. Demissie, C.H. Sime, Assessment of the performance of CORDEX regional climate models in simulating rainfall and air temperature over southwest Ethiopia, Heliyon 7 (8) (2021) e07791.
[25] I. Garba, Z.S. Abdourahamane, Extreme rainfall characterisation under climate change and rapid population growth in the city of Niamey, Niger, Heliyon 9 (2) (2023) e13326.

[26] U. Pawar, S. Try, N. Muttil, U. Rathnayake, W. Suppawimut, Frequency and trend analyses of annual peak discharges in the Lower Mekong Basin, Heliyon 9 (9) (2023) e1690.
[27] C.H. Sime, W.T. Dibaba, Evaluation of CMIP6 model performance and extreme precipitation prediction in the Awash basin, Heliyon 9 (11) (2023) e21578.
[28] I. Ahmad, et al., Estimation of regional and at-site quantiles of extreme winds under flood index procedure, Heliyon 10 (1) (2024) e23388.
[29] I. Ahmad, T. Ahmad, S.U. Rehman, I.M. Almanjahie, F. Alshahrani, A detailed study on quantification and modeling of drought characteristics using different copula families, Heliyon 10 (3) (2024) e25422.
[30] R.T. Cooper, Projection of future precipitation extremes across the Bangkok metropolitan region, Heliyon 5 (5) (2019) e01678.
[31] C.M. Tfwala, et al., Nationwide temporal variability of droughts in the Kingdom of Eswatini: 1981–2018, Heliyon 6 (12) (2020) e05707.
[32] D. Naeem, R. Aziz, M. Awais, S.R. Ahmad, Assessment of historical and projected changes in extreme temperatures of Balochistan, Pakistan using extreme value theory, Environ. Monit. Assess. 196 (4) (2024) 375.
[33] A.K. Mishra, V.P. Singh, Changes in extreme precipitation in Texas, J. Geophys. Res. Atmos. 115 (D14) (2010).
[34] D. She, et al., Investigating the variation and non-stationarity in precipitation extremes based on the concept of event-based extreme precipitation, J. Hydrol. 530 (2015) 785–798.
[35] K.L. Ebi, K. Bowen, Extreme events as sources of health vulnerability: drought as an example, Weather Clim. Extrem. 11 (2016) 95–102.
[36] M. Beroho, et al., Analysis and prediction of climate forecasts in Northern Morocco: application of multilevel linear mixed effects models using R software, Heliyon 6 (10) (2020) e05094.
[37] H. Desalegn, A. Mulu, Mapping flood inundation areas using GIS and HEC-RAS model at fetam river, upper abbay basin, Ethiopia, Sci. African 12 (2021) e00834.
[38] S. Du, et al., Projection of precipitation extremes and flood risk in the China–Pakistan economic corridor, Front. Environ. Sci. 10 (2022) 887323.
[39] R. Verma, S.C. Rai, Evaluation of spatio-temporal variability of a flood using the hydrological process of flood frequency in ghagra river basin, India, J. Geol. Soc. India 99 (12) (2023) 1671–1682.
[40] W.H. Hassan, B.K. Nile, Z.K. Kadhim, Effect of climate change on the flooding of storm water networks under extreme rainfall events using SWMM simulations: a case study, Model. Earth Syst. Environ. (2024) 1–33.
[41] S. Yildiz, H.M.T. Islam, T. Rashid, A. Sadeque, S. Shahid, M. Kamruzzaman, Exploring Climate change effects on drought patterns in Bangladesh using bias-corrected CMIP6 GCMs, Earth Syst. Environ. 8 (1) (2024) 21–43.
[42] A. Lenouo, D. Monkam, D.A. Vondou, R.S. Tanessong, F.M. Kamga, Analyse des conditions météorologiques pour la sécurité aérienne à Douala, Meteorol. 2009 (65) (2009) 46–58.
[43] D. Sighomnov, S. Nkamdjou, G. Tanyileke, Les fortes pluies de la région du mont Cameroun: le cas d'Idenau, Météorologie (2) (1993) 41–47.
[44] R.S. Tanessong, D.A. Vondou, Z.Y. Djomou, P.M. Igri, WRF high resolution simulation of an extreme rainfall event over Douala (Cameroon): a case study, Model. Earth Syst. Environ. 3 (2017) 927–942.
[45] U. Schneider, D. Henning, H. Hauschild, M. Reiss, B. Rudolf, Zur Berechnung monatlicher Niederschlagshöhen aus synoptischen Meldungen, Meteorol. Z. (1992) 22–31.
[46] U. Schneider, Receipt of SYNOP reports at DWD during the period 1986-2005 and the temporal coverage of accumulated monthly precipitation totals, Europe 1001 (2005) 19998.
[47] D. Ndarwe, D. Bongue, D. Monkam, P. Moudi, N. Philippon, C.A. KenfacK, Analysis of the diurnal to seasonal variability of solar radiation in Douala, Cameroon, Theor. Appl. Climatol. 138 (2019) 249–261.
[48] I.C. Enete, M.E. Awuh, F. Ikekpeazu, Assessment of urban heat island (uhi) situation in Douala metropolis, Cameroon, J. Geogr. Earth Sci. 2 (1) (2014) 55–57.
[49] A. Kemajou, A. Tseuyep, N.E. Egbewatt, Le confort thermique en climat tropical humide vers un réaménagement des normes ergonomiques, J. Renew. Energies 15 (3) (2012) 427–438.
[50] M.K. Nematchoua, G.R. Roshan, R. Tchinda, T. Nasrabadi, P. Ricciardi, Climate change and its role in forecasting energy demand in buildings: a case study of Douala City, Cameroon, J. Earth Syst. Sci. 124 (2015) 269–281.
[51] A. David, N.R. Ngwa, Global Solar Radiation of some regions of Cameroon using the linear Angstrom and non-linear polynomial relations (Part I) model development, Int. J. Renew. Energy Resour. 3 (4) (2013) 984–992.
[52] M. New, et al., Evidence of trends in daily climate extremes over southern and west Africa, J. Geophys. Res. Atmos. 111 (D14) (2006).
[53] E.J. Gumbel, Les valeurs extrêmes des distributions statistiques, in: Annales de l'institut Henri Poincaré, 1935, pp. 115–158.
[54] S. Coles, J. Bawa, L. Trenner, P. Dorazio, An Introduction to Statistical Modeling of Extreme Values, vol. 208, Springer, 2001.
[55] R. Chamani, D. Monkam, Z.Y. Djomou, Return times and return levels of July–September extreme rainfall over the major climatic sub-regions in Sahel, Atmos. Res. 212 (2018) 77–90.
[56] R.L. Smith, Statistics of extremes, with applications in environment, insurance, and finance, Extrem. values Financ. Telecommun. Environ. (2003) 20–97.
[57] A.C. Davison, Statistical Models, vol. 11, Cambridge university press, 2003.
[58] J. Grela, M.A. Nowak, On relations between extreme value statistics, extreme random matrices and Peak-Over-Threshold method, arXiv Prepr. arXiv1711.03459 1711 (2017).
[59] J. Pickands III, Statistical inference using extreme order statistics, Ann. Stat. (1975) 119–131.
[60] R.L. Smith, Threshold methods for sample extremes, in: Statistical Extremes and Applications, Springer, 1984, pp. 621–638.
[61] J. del Castillo, D.M. Soler, I. Serra, M.I. Serra, Package 'ercv, 2019.
[62] K. Born, A.H. Fink, H. Paeth, Dry and wet periods in the northwestern Maghreb for present day and future climate conditions, Meteorol. Z. 17 (5) (2008) 533.
[63] A.A. Balkema, L. De Haan, Residual life time at great age, Ann. Probab. 2 (5) (1974) 792–804.
[64] J.R.M. Hosking, J.R. Wallis, Parameter and quantile estimation for the generalized Pareto distribution, Technometrics 29 (3) (1987) 339–349.
[65] R.L. Smith, Extreme value analysis of environmental time series: an application to trend detection in ground-level ozone, Stat. Sci. (1989) 367–377.
[66] R. Chamani, D. Monkam, Z.Y. Djomou, Analysis of return periods and return levels of yearly july–september extreme droughts in the west african sahel, Clim. Dynam. 52 (5) (2019) 3421–3433.
[67] D.F. Hendry, L.R. Klein, A textbook of econometrics, Econ. J. 84 (335) (1974) 688, https://doi.org/10.2307/2231072.
[68] E.L. Molua, Climatic trends in Cameroon: implications for agricultural management, Clim. Res. 30 (3) (2006) 255–262.